SPAWAR CST/LLFA-RPT-EVA-9A

Reassessing the Issue of Pulse-Length Dependence of Bottom Scattering Strengths in Critical Sea Test Data

September 1996

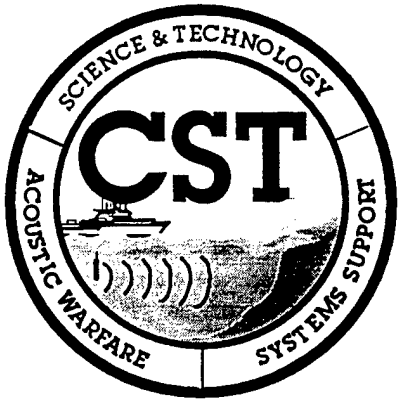

By:
Roger C. Gauss[1], Joseph M. Fialkowski[2],
Frank S. Henyey[3], Peter M. Ogden[1],
Sean M. Reilly[4], Michael T. Sundvik[4], and Eric I. Thorsos[3]

Prepared for:
Space and Naval Warfare Systems Command (PMW-182)

Naval Research Laboratory, Washington DC[1]
Planning Systems, Incorporated, McLean VA[2]
Applied Physics Laboratory, University of Washington, Seattle WA[3]
Naval Undersea Warfare Center, Newport RI[4]

Executive Summary

During the course of the Critical Sea Test (CST) program, a substantial number of measurements have been made of low-frequency, direct-path bottom scattering using both SUS charges and controlled waveforms. An unexpected pulse-length dependence (PLD) of low-frequency, bottom-scattering strengths (BSS) was reported to have been observed in some coherent source data collected in several CST-5 and CST-7 Phase-3 locations. This dependence was basically independent of grazing angle and almost exclusively seen at frequencies between 875 and 1010 Hz. (Different signals were used across the tests. In a given run, the two signals with different pulse lengths also had different center frequencies.) However, such a dependence of scattering strength on pulse length contradicts basic theory, barring an unlikely sharp resonance in the dominant bottom-scattering mechanism. A review of the original processing and results, as well as independent reprocessing of selected CST-5 data revealed the reported PLDs to be due primarily to two effects: (1) a misapplication of intended source levels into the sonar-equation–based programs that compute scattering strengths (a ~4-dB, time-independent error); and (2) an error in how time was converted to grazing angle in these programs (up to ~2-dB, mildly time-dependent error). These adjustments are generally consistent with the observed grazing-angle independence of the BSS's. Additionally, differences were found between the original and reprocessed absolute reverberation levels and the range of valid times (grazing-angle coverage).

Due to near-field effects, *apparent* PLD effects can be observed in acoustic field data: longer pulses and greater decay rates can both bias scattering strengths upward when estimated with the standard algorithm. However, straightforward formulas have been developed to correct for these biases. It should be noted that this correction does *not* require any knowledge of the subbottom or the system used to collect the data. To support prediction capabilities for active systems, it is recommended procedures be identified for realizing such corrections for *apparent* pulse-length–dependent effects at the operational level. (At a minimum, operators should be made cognizant of the phenomena.) Two such procedures include either:

> Simulating (apparent) pulse-length effects when generating model curves for prediction or comparison with data curves (e.g., running a "T-second" window over the predicted RL curve of an impulsive signal),

or

> Correcting the data curves and then comparing them with model predictions of impulsive signals (e.g., to invert for bottom parameters).

THE BOTTOM LINE is that **the pulse length dependence of bottom scattering strengths is no longer an issue.**

Reassessing the Issue of Pulse-Length Dependence of Bottom Scattering Strengths in CST Data

ABSTRACT

During the course of the Critical Sea Test (CST) program, a substantial number of measurements have been made of low-frequency, direct-path bottom scattering using both SUS charges and controlled waveforms. An unexpected pulse-length dependence (PLD) of low-frequency, bottom-scattering strengths (BSS) was reported to have been observed in some coherent source data collected in several CST-5 and CST-7 Phase-3 locations. This dependence was basically independent of grazing angle and almost exclusively seen at frequencies between 875 and 1010 Hz. (Different signals were used across the tests. In a given run, the two signals with different pulse lengths also had different center frequencies.) However, such a dependence of scattering strength on pulse length contradicts basic theory, barring an unlikely sharp resonance in the dominant bottom-scattering mechanism. A review of the original processing and results, as well as independent reprocessing of selected CST-5 data revealed the reported PLDs to be due primarily to two effects: (1) a misapplication of intended source levels into the sonar-equation–based programs that compute scattering strengths (a ~4-dB, time-independent error); and (2) an error in how time was converted to grazing angle in these programs (up to ~2-dB, mildly time-dependent error). These adjustments are generally consistent with the observed grazing-angle independence of the BSS's. Additionally, differences were found between the original and reprocessed absolute reverberation levels and the range of valid times (grazing-angle coverage). The bottom line is that pulse length dependence of bottom scattering strengths is no longer an issue.

1. INTRODUCTION

An unexpected pulse-length dependence (PLD) of low-frequency, bottom-scattering strengths was reported to have been observed in some coherent source data collected in several Critical Sea Test (CST) locations (Reilly *et al.* 1995a, 1995b). For a given data set, the waveforms in question were interleaved upon transmission so that, on average—the results were ping averaged—they each experienced the same environment. However, this PLD contradicts basic theory, barring an unlikely sharp resonance in the dominant bottom-scattering mechanism (Henyey *et al.* 1995, 1996). The primary focus of this report is determining the validity of the processed results.

The processing and published results from selected CST runs have been reviewed, and the acoustic data independently reprocessed, with the goal of seeing if the results are reproducible and ascertaining the reasons if not. As the same source/receiver system, recording and processing were used for virtually all the CST coherent-pulse data analysis (save CST-8, where the effect was not seen), if the results for any one experiment can be verified then a phenomenon of major importance has been discovered. If, on the other hand, the results cannot be verified and, moreover, are shown to be pulse-length *independent*, then the theoreticians and system designers may sleep a little easier.

2. REVIEW OF RELEVANT DATA

During the course of the CST program, high-quality acoustic measurements using both impulsive and controlled waveforms characterized bottom backscattering as a function of frequency, geometric parameters (such as grazing angle) and environmental parameters (such as bottom type). Field testing revolved around the research vessel (R/V) *Cory Chouest*. This dedicated,

well-outfitted platform collected data throughout the northern hemisphere. Both impulsive and controlled sources were used not only to establish the connection between results using explosive charges and the waveforms of operational interest, but to unravel the physics behind the empirical results.

These highly-specialized EVA measurements were primarily monostatic measurements, conducted as a small number of short (30-min to 2-hr) modules interleaved among more system-oriented measurements. (Each execution of a module is known as a "run," generally indexed chronologically within a given sea test.) Using a small number of modules, repeated often, allowed a good sampling of environmental conditions (e.g., bottom-scatter data collected in different locations). Within a module, a small number of signals (typically, 1 to 10) were transmitted often—typically, every 60 to 180 s for short-range (or "direct-path") measurements—to provide meaningful statistics when comparing the results of one run versus another.

For the CST controlled-waveform results discussed in this report, the experimental configuration typically consisted of a 128-element, horizontal line array, cut for 1 kHz, as a receiver—known as the "high-frequency" array or HFA—towed roughly 1 km aft of the ship, and a series of contiguous vertical line arrays (VLAs) (deployed at midships through a center well) of 10 to 20 high-level sources (in each of three frequency bands: LF, 190-310 Hz; MF, 350-450 Hz; and HF, 850-1100 Hz, with typical individual element source levels of 213, 208 and 203 dB re 1μPa @ 1 m, respectively). (The three source arrays could all be operated simultaneously.) The sources and the receiver were both normally towed at center depths between 100 to 200 m at 3 kt. Both narrowband (Continuous Wave [CW]) and broadband (Hyperbolic Frequency Modulation [HFM]) transmissions of various bandwidths and durations were used. For direct-path bottom-scattering measurements, signal durations ranged between 0.05 and 4 s.

Significantly, the VLA sources were steerable and allowed application of shadings—such as Hamming and Taylor—to control sidelobe energy. These capabilities were exploited particularly during the direct-path, bottom-scattering measurements described here, where the source arrays were both shaded and steered down between 20 and 30 deg. This allowed obtainment of low-grazing–angle data by both ensonifying the bottom (steering down) and suppressing high-angle ensonification of the receiver sidelobes (shading).

For more details on both the experimental techniques and equipment used in CST, see Vaccaro *et al.* 1996.

2.1 CST-5 through CST-8

Bottom-scattering strengths (BSS) were derived from coherent source data collected in a number of CST-5, -7 and -8 locations within the LF, MF and HF source bands. An overview of experimental results is presented in Reilly *et al.* (1995a). More detail on experimental methods, processing methodologies, at-sea operations and the local geophysics for the individual tests may be found in Reilly and Sundvik (1992), Reilly and Craig (1993) and Reilly (1994). In the following we concentrate on just those runs where data corresponding to waveforms of different pulse lengths have been analyzed for BSS and the findings reported.

CST-5

HF tests were conducted in the spring of 1991 in the Ionian Sea, both in a deep basin (Run 1B) and in shallow water along the edge of a steep escarpment (Run 44). These runs provided the clearest examples of PLD (Reilly and Sundvik 1992; Reilly *et al.* 1995a): Fig. 1 shows separations of ~7–8 dB (1- and 0.25-s CW data from Run 1B, Ionian Basin) and ~4–5 dB (0.1- and 0.05-s CW data from Run 44, Medina Bank). (No HFMs were processed.) Note that in each case, the longer duration pulse has the greater BSS, and that the PLD effect is basically independent of grazing

angle. It is important to note that the CWs have different frequencies—see Table 1: the 1-s CW was at 880 Hz, the 0.1-s CW was at 1004 Hz, while the 0.25- and 0.05-s CWs were both at ~935 Hz.

CST-7 Phase 3

MF and HF bottom scattering tests were performed in the spring of 1992 in four environments near the edge of the continental shelf in the vicinity of the Quinalt Canyon off the coast of Washington during CST-7 Phase 3. These were designated as the north shelf (Run 12), the slope (Run 13), the canyon (Run 21) and the south shelf (Run 17). The reported PLD results (Reilly and Craig 1993; Reilly *et al.* 1995a) were decidedly less marked than those seen in CST-5 at HF, and generally inconsistent at MF:

HF. Fig. 2 shows that the 0.25-s HFM BSS's are on average noticeably greater than the CW BSS's (by ~3 dB). However, in the one case where both the 0.10- and 0.05-s CWs are present (Run 17), no clear separation between them is noted (in contrast to CST-5 Run 44). Again note that the CWs have different frequencies: the 0.1-s CW was at 1004 Hz, while the 0.05-s CW was at 935 Hz.

MF. At MF, there was no general pulse-length character to the BSS's. (Again, the very short-duration signals were at different frequencies—see Table 1.) Fig. 3 shows examples where PLD was *not* seen: in one case (Run 13, slope), the order of strength is 0.05, 0.25 and 0.10 s, while in the other case (Run 21, canyon), the order is 0.10, 0.25 and 0.05 s. The separation in either case between all the curves is at most a few dB. There was one MF case (Run 12, north shelf) where a PLD of ~4.6 dB was reported (Table 3-4 in Reilly and Craig 1993), though no corresponding plot showing the grazing-angle dependence was published in this reference. However, for this run it is most interesting to note the extreme spatial variability of the MF BSS's in this location: Fig. 3-7 of Reilly and Craig (1993) shows a ~16-dB change in BSS for the 0.1-s CW within 30 min.

CST-8

LF and HF bottom scattering tests were conducted in the spring of 1993 in the Nile Fan during CST 8. No PLD was noted at either LF or HF in CST-8 locations (Reilly 1994). The data collected here used a different source (omni) and source platform than those in CST-5 and CST-7 Phase 3. Further details on the experimental results may be found in Reilly (1994).

Summary of key points

- Same system and processing used for all CSTs (except CST-8).
- Different signals were used across the tests—see Table 1. For example, at HF: 0.25-s, 936-Hz and 1-s, 880-Hz CWs in deep water (CST-5), and 0.05-s, 935-Hz and 0.1-s, 1004-Hz CWs in shallow water (CST-5 and CST-7 Phase 3).
- PLD reported to be observed in some areas (CST-5 locations) and not at all in others (CST-8 locations).
- With the same pair of signals, PLD was seen in CST-5 Run 44, but not in CST-7 Phase 3 Run 17.
- PLD seen in some CST frequency bands and not in others:
  - Mainly HF (only exception CST-7 North Slope MF).
  - Never below 345 Hz.

  If this is a bottom-interaction phenomenon, one might expect it also to manifest itself at

lower frequencies. Potential reasons for its absence at these frequencies are: (1) it could relate to some small-scale phenomenon that longer wavelengths are not sensitive to; and (2) the scattering process may be dominated by scatterers sufficiently deep in the subbottom that they are not reached by the HF signals at the angles ensonified.

- Where seen, longer pulses have the greater BSS's— in these cases, the ΔBSS is roughly $10\log(T_{longer}/T_{shorter})$, i.e. $10\log T + const$, where T is the pulse length (Reilly *et al.* 1995a).
- Where seen, the PLD has basically no dependence on grazing angle.
- Not all relevant CST data have been processed.

2.2 Other experiments

Signals of varying pulse lengths have been transmitted in other SPAWAR bottom-scattering experiments (also using the R/V *Cory Chouest*). No PLD effects have been observed in the data processed to date:

Magellan I. LF data collected, but not yet analyzed.

CST-10/Magellan II. Not seen in LF data processed so far (Holland, PSI, personal communication 1996). HF data exists, but have not yet been processed for BSS.

LFA-11. Not seen after processing an extensive collection—35 sites—of LF data.

LFA-13. LF data collected, but not yet analyzed at multiple pulse lengths.

2.3 Sea surface scattering results

For low-frequency (< 1000 Hz) sea-surface scattering strengths (SSS), no such pulse-length dependence has been observed in CST data (Ogden and Gauss 1996). General agreement has been observed between SSS's derived from both impulsive—SUS charges—and controlled waveforms (0.05- to 2.4-s CWs and LFMs, and by inference, 12-s Hanned CWs).

3. REVIEW OF THEORY

A theoretical analysis shows that the "ideal" scattering strength is independent of pulse length or pulse type for two pulses with the same carrier frequency (Henyey *et al.* 1995, 1996). The ideal scattering strength is obtained for pulses with narrow enough bandwidth that one can completely neglect the frequency dependence of the scattering strength over that of bandwidth. The measured scattering strength is an average of the ideal scattering strength over the frequency band of the pulse. The demonstration of the pulse-length independence is based on well-founded assumptions.

3.1 Assumptions

The assumptions are:

- The pressure field obeys a linear wave equation.
- The environment is independent of time, and ship-motion effects have been removed.
- The scattering strength is slowly varying over the bandwidth of the pulse.

3.2 Summary of the argument

Any source pulse $s(t)$ can be written as $s(t) = \int s(\tau)\delta(t-\tau)d\tau$. Then the principle of superposition tells us that the pressure at the receiver $P(t)$ from an arbitrary pulse is the response from a delta function pulse (the impulse response function) convolved with $s(t)$. Fourier transforming into the frequency representation turns this convolution into a product; $\tilde{P}(f) = \tilde{s}(f)\tilde{k}(f)$, where $\tilde{s}(f)$ and $\tilde{k}(f)$ are the Fourier transforms of $s(t)$ and the impulse response function, respectively. The absolute square of this expression, integrated over frequency, is $E_r = E_s < |\tilde{k}|^2 >$, where E_r is proportional to the energy returned, where E_s is proportional to the source energy, and where the angle brackets indicate an average weighted by the spectrum $|\tilde{s}(f)|^2$ of the transmitted waveform. The factor $< |\tilde{k}|^2 >$ is independent of the pulse, except for its relative frequency content. The third assumption allows us to replace this average by $|\tilde{k}|^2$ at the nominal carrier frequency.

In the remainder of the demonstration, the sonar equation is used to show that, in essence, the scattering strength depends only on $< |\tilde{k}|^2 >$. The sonar equation involves the ensonified area, which is proportional to the pulse length, and the transmitted power. Together, these make the transmitted energy, which cancel the factor of E_s in the above expression when the scattering strength is calculated. There is no remaining reference to the source pulse, other than its nominal frequency. In particular, the pulse length is irrelevant. The details of the derivation are contained in Henyey *et al.* 1996.

3.3 Implications for experiments

For typical CW pulses, the frequency dependence of the scattering strengths over the pulse bandwidth should be negligible, i.e. the third assumption above applies, and scattering strength independent of pulse length will result. If, on the other hand, two pulses have a very large bandwidth difference, e.g., hundreds of Hz, the third assumption may not apply, and then some difference in scattering strength with pulse type would not be inconsistent with the analysis. In addition, if the center frequency of two pulses differ, the intrinsic frequency dependence of the bottom scattering strength may be observed in the measurements. In general, however, there is only modest frequency dependence for low-frequency bottom scattering: a 6-dB change in scattering strength over a factor of 2 change in frequency would be in the high range (Ogden, personal communication 1996). For the CST-5 results analyzed in detail in this report (Fig. 1a), the pulse lengths (CW) were 0.25 s and 1.0 s at 936 Hz and 880 Hz, respectively—see Table 1. The 56-Hz difference in center frequency for these two pulses could in principle lead to measured scattering strength differences, without conflicting with the theoretical analysis. However, significant scattering strength differences between these two frequencies would be highly unexpected based on past measurements of the frequency dependence of bottom scattering. Very uniform layering in the sediment, for example, could lead to significant scattering strength variations over a 50-Hz frequency difference in the vicinity of 900 Hz. However, a rapid oscillatory variation of the scattering strength with grazing angle would also be expected (D.R. Jackson, APL/UW, personal communication 1995; see also Fig. 3 in Moe and Jackson 1994). Such dependencies were not observed in these low-frequency experiments (Holland *et al.* 1996a).[1] For the CST-5 data, the nominal bandwidths of 4 Hz and 1 Hz are sufficiently small that the third assumption above should be exceedingly well satisfied. Thus, if bottom scattering strengths were measured with these pulses at the same center frequency, agreement in measured scattering strength for the two pulse lengths is predicted with extremely high confidence.

[1] Oscillations in grazing angle have been seen by the lead author (Gauss *et al.* 1996) in the 190-to-310 Hz BSS data from LFA-11 (on the Scotian Continental Rise), but no dependence of BSS on pulse length was seen using CW and HFM signals of durations ranging from 0.1 to 4 s.

4. TOWARDS RESOLUTION OF THE CONTROVERSY

4.1 Goals and methods of investigation

To investigate the pulse-length dependence of bottom-scattering strength reported to have been observed in some of the CST data, an effort has been made to independently reproduce the reported results. The purpose was not to reprocess all the data, but to verify the input parameters and assumptions, the processing methodology and the sonar-equation values obtained as both reasonable and accurate.

To this end, the most notable case, HF Run 1B from CST-5—see Fig. 1a—was chosen.[2] Furthermore, Run 1B was a deep-water case, allowing for simpler investigation and surer interpretation of the sonar-equation terms vs. time.

Before examining that run in detail, we address some more general issues:

4.2 Source level (SL)

One potential source of discrepancy was uncovered in that the "typical" single-element source-frequency curves for HF—e.g., Dubord *et al.* (1990)—turned out not to be so typical after all. Reilly used the curve reported as representative in Dubord *et al.* (1990)—solid curve in Fig. 4. However, in another well-referred-to document,[3] a different curve is presented as "typical," namely, the dashed curve in Fig. 4. As can be seen, there is a difference of 30 Hz between the locations of their (first) peak resonances. Consequently, an attempt was made to clarify HF source levels. The Seneca-Lake calibration of the individual HF elements—Dubord *et al.* (1990)—was used to derive (linear) average HF SL-vs-frequency values, the solid curve in Fig. 5. The resultant average displayed a broader resonance than either of the "representative" curves, with increased SL over the lower frequencies of the source band. This newly-derived curve was then verified to the extent possible:

- First, an attempt was made to confirm the frequency character of this mean curve. Direct arrivals of broad bandwidth (240-Hz) Linear Frequency Modulated (LFM) signals (from CST-7 Phase-2) recorded on the forward desensitized hydrophone (Fwd DeSen phone) were used. Correcting these spectra for the hydrophone's sensitivity versus frequency as measured at sea, though unfortunately only possible between 900 and 1100 Hz—see author for reference—excellent agreement with the above-mentioned resultant mean curve was obtained—see dashed curve in Fig. 5.

- Next, an attempt was made to determine the absolute SL. (The first step just gave the shape of the frequency-response curve—no attempt was made to back out TL, etc. to determine absolute SLs.) For this, the mean curve was compared with both Seneca-Lake and at-sea SL measurements. The most confidence was placed in the Seneca-Lake measurements—the conditions were much more controlled—and included both source array and single-element measurements, though unfortunately the former were only at one frequency. Additionally, whenever available, SLs recorded during CST at-sea calibrations were used as well to help estimate what the "true" SLs were.

[2]Notation: Reilly and Sundvik (1992) (and Reilly *et al.* 1995a) break Run 1B into sub-runs: e.g., Runs 1H and 1I occur simultaneously, but the former corresponds to the 1-s CW data and the latter to the 0.25-s CW data.

[3]See author for reference.

As a result of these comparisons, the conclusion was: use the newly-derived single-element mean curve and subtract an additional 0.8 dB. This extra adjustment comes from finding a 0.8-dB degradation of the measured *array* SLs relative to the single-element SLs + $20 \log N$, where N was the number of source-array elements. Specific single-element SLs include: 202.8 dB @ 880 Hz, 201.9 dB @ 935 Hz, 199.8 dB @ 1004 Hz and 201.4 dB over 900-1000 Hz.

A similar exercise at MF was performed: all the individual elements were *very* similar to one another—in sharp contrast to HF. See Figs. 6 and 7. (These curves have yet to be compared with direct arrivals of LFMs on the Fwd DeSen phone.)

4.3 Timing

In recent investigations of surface scattering strengths, some subtleties in timing, i.e. conversion of time to mean grazing angle, for non-impulsive signals have been resolved (Gauss *et al.* 1995). It has been seen to be of significance in deriving SSS's even for CWs with durations as short as 0.25 s (Gauss *et al.* 1995). Furthermore, *errors of one pulse length in referencing time were recently found* by Sundvik and Chester (NUWC) in deriving CST-7 SSS's from 0.05-s and 0.25-s CWs *using the same processing stream* as used in the original BSS processing (Chester, personal communication 1996). A careful attempt was made to see if timing errors could be the source of any of the pulse-length dependence observed in the CST bottom scattering strengths.[4] As will be shown later, it turned out to be one of the two factors responsible for the reported PLD of the CST-5 Run-1B BSS's—see Section 6.9.

5. CST-5 RUN 1B: REVIEW OF THE INPUT PARAMETERS

To determine that the derivation of the sonar-equation terms for CST-5 Run 1B was as accurate as possible, attempts were made both to confirm the original choices of the input parameters and to determine their sensitivity to reasonable choices of their values. The parameter choices used in both the original processing and in the reprocessing are summarized in Table 2.

5.1 Sound-speed profile

The sound-speed profile (SSP)—derived from XBT Cast 1009—assumed in the reprocessing was the same used in the original processing of the CST-5 Run-1B data.[5] It was found to be virtually identical to SSPs taken both 2 hours prior and 2 hours later.

5.2 Source tilt

A source tilt of 3.5° may be more reasonable, but to match the original processing a tilt of 4° was assumed. (It will be shown later that BSS *levels* were relatively insensitive to reasonable choices of source tilt for the beams considered in this study.)

5.3 Source-receiver separation

The backscattered signals were received on the HFA. Using documented values of cable scope (860 ft = 262.1 m), source depth, receiver depth, source tilt, and the *in situ* sound speed, the horizontal projection of the distance from the center of the source array to the Fwd DeSen phone was calculated to be 828 m. This calculated distance was verified using time-of-flight measurements of the 0.25-s CWs to the Fwd DeSen phone: consistent timings of ~0.55 s put its distance from

[4] *Aside*: When simultaneously transmitting in different frequency bands (e.g., LF and HF) with the R/V *Cory Chouest*'s VLA, one must look at the "non-TCB" signal on a ping-by-ping basis to determine the exact transmission time. While the delays might "average out" to some nominal value (say, 0.070 s), the effect on timing will be greater the shorter the signal's duration. This mode of transmission was not used by Reilly in CST 5 or CST-7 Phase 3.

[5] The same SSP was used in processing the immediately–prior, Run-2 SUS data for scattering strengths.

source at 833 m. The distance from this phone to the head of the HFA is 14.9 m. As the spacing between HFA elements is 0.76 m, the distances to the middle of receiving subapertures used in the original processing (phones 23 to 105) and in the re-processing (phones 23 to 86), would be 890.9 and 883.8 m, respectively. The original processing assumed 880.1 m, and 880 m was used here.

5.4 Near-field considerations

Using D^2/λ as a criterion, any HFA subaperture of 106 m or less can be used for the CST-5 deep-water sites as the range D where valid data exist is 7500 m or greater (for the aft beams examined here). As the entire HFA is 100 m long, there is no problem using *any* HFA subaperture for processing CST-5 deep-water, aft-beam BSS's. (Aside: for the Run-1B data examined here, the bottom depth was ~3400 m.)

5.5 Data-processing: general methodology

The original processing used Hamming-weighted beamforming—these beams were formed at sea by the real-time processor (RTP) (Sundvik, personal communication 1996).[6] The reprocessing worked directly from the high-density digitally recorded (HDDR) element data. These HDDR data were conventionally filtered and beamformed with normalized Hamming weighting, correcting for the directionality of the hydrophone groups at HF: 0 dB at broadside, +0.8 dB at 138°R, +1.5 dB at endfire.

CW processing

The original processing used a time-domain, Hanning-weighted IIR filter. These narrowband filter bandwidths were set to 3 times the signal's natural bandwidth, i.e. 3 Hz for the 1-s CW and 12 Hz for 0.25-s CW (Reilly and Sundvik 1992).

The reprocessing used conventional FFT-based methods to produce power spectral densities (PSD) as a function of time. Here, windows were matched to the pulse duration (with 90%-overlap between windows). The PSDs were then summed over frequency bands keyed to the pulse duration to give the total power. To match the original processing, we used 3- and 12-Hz bands for the 1- and 0.25-s signals, respectively. We also increased these to 8- and 24-Hz bands, respectively, which increased the RLs by less than 0.2 dB. (See Fig. 8 for representative spectra.)

In both cases, ownship motion is accounted for at this stage.

All 12 pairs of 1- and 0.25-s CW pings from ping times 161 0217–0241 Z were used in the reprocessing. The original processing used 12 1-s and 19 0.25-s CW pings to compute their averages.

HFM processing

In both the original processing and the reprocessing methods, HF HFM data are match-filtered prior to sonar-equation analysis. None of the HFM data collected in CST-5—see Table 1—were originally processed for BSS. However, during the reprocessing, BSS's were derived from these data.

[6] For a test case, BSS's were derived from SUS data using both RTP beam data and post-test beamformed data using the raw hydrophone data. No systematic offsets were found using the two methods.

6. CST-5 RUN 1B: THE SONAR EQUATION TERM-BY-TERM

The sonar-equation formulas used in calculating the scattering strengths are given by:

$$BSS_{CW} = RL - SL + TL_{out} + TL_{back} - 10\cdot\log(A)$$
$$BSS_{FM} = RL - SL + TL_{out} + TL_{back} - 10\cdot\log(A) + 10\cdot\log(W),$$

where BSS is the desired bottom scattering strength in dB, RL is the observed reverberation level in dB re $(1\ \mu\text{Pa})^2$, SL is the source level in dB re 1 μPa at 1 m, TL_{out} is the one-way transmission loss from the source to the scattering patch, TL_{back} is the one-way transmission loss from the scattering patch to the receiver, A is the area of the scattering patch in m^2, and W is the bandwidth of the FM waveform in Hz. (Flat-bottom scattering off the interface is assumed.) Adjustments are required for the CW signals to account for the finite pulse length and the finite temporal resolution of the receiver (Gauss *et al.* 1995; Henyey *et al.* 1995, 1996)—see the Appendix for an adjustment formula (from Gauss 1996). Additionally, as noted earlier, the longer the CW pulse length, the more important it is to use the correct timing.

Linear averaging over pings was done to determine the mean response for individual beams: for both the original processing and the reprocessing, this averaging was over RLs.

Printouts of various direct-path processing input parameters and output values as a function of time for the 138°R beam are displayed as Figs. 9 and 10 for the original processing and the reprocessing, respectively, for both the Run-1B, 1- and 0.25-s CWs. These detail how the inputs to the sonar equation generated by the two processing methods compare. To provide a quick overview of how various terms vary with time, Fig. 11 shows the mean grazing angle, 2-way TL, A and SL-adjustment vs. time, as calculated in the *reprocessing* of the 138°-R–beam BSS's. For this method, valid times are defined as those when the ensonified patch remains within 3 dB of the beams' main-response axes (MRAs).

WE NOW EXAMINE BOTH THE ORIGINAL AND THE REPROCESSED DATA TERM-BY-TERM:

6.1 RL – NL

In the sonar equation, the RL computed is really RL – NL, where NL is the Noise Level. However, as the beam-noise levels were negligible relative to the reverberation levels over valid times for the beams considered here, i.e. RL – NL ≈ RL, we will simply denote RL – NL as RL for the rest of this report. (For both processing schemes, there is a minimum criterion that RLs must be at least 3 dB above the NL for a time to be considered as "valid" for computing BSS's.)

Original processing

The RL-vs.-time curves for the two CW signals are shown in Fig. 12.

Reprocessing

The RL-vs.-time curves for the two CW signals are shown in Fig. 13. As a check, we examined whether their background levels scaled 6 dB as expected given their different widths of integration over frequency (3 Hz vs. 12 Hz). Averaging over pings and over time periods corresponding to ambient conditions (10 to 5 s prior to the first transmission), they indeed did. (This cannot be seen in Fig. 13 as the 1-s–CW RL is still decaying into the noise at 50 s—see the small zero-Doppler component of the noise curve in Fig. 8a, which represents an average over 40 to 50 s after transmit.) We also checked the effect of widening the frequency-integration bands to 8 Hz for the 1-s CW and

to 24 Hz for the 0.25-s CW. In each case, the difference in widening the band of integration resulted in an increase of ~0.2 dB. (This adjustment was *not* included in the computed BSS's.)

Comparison

The reprocessed RLs differ considerably from those of the original processing—see Table 3 for representative values. First, for either signal, the *absolute* RLs derived from the two processing methods do not agree: for the 1-s CWs, $RL_{repro} - RL_{orig} \approx 5.6$ dB; while, for the 0.25-s CWs. $RL_{repro} - RL_{orig} \approx 7.2$ dB. Secondly, by processing scheme, the RLs of the 1-s CWs *relative* to those of the 0.25-s CWs differ by ~11.7 dB in the original processing and by ~10 dB in the reprocessing. The latter differences are likely due to how the two processing methods referenced time (relative to ping transmit)—see Section 6.9.

In studying why the absolute levels do not agree, normalization procedures were examined. In the original processing, two weightings were applied: Hamming in the beamforming and Hanning in the CW filter. The direct-path programs assume unity beamforming. So, if weights are not normalized in the beamforming, then a correction must be applied to the RL, e.g., +5.35 dB for Hamming and +6.02 dB for Hanning.[7] *However*, Sundvik (personal communication, 1996) reports normalization not to be a problem; in fact, a comparison of NRL- and NUWC-derived CST-7 Phase-2 surface scattering strengths revealed virtually identical SSS's *and* RLs. Thus, THE ABSOLUTE HF CST-5 RUN-1B RL DIFFERENCES REMAIN A MYSTERY AT THIS TIME. (The only avenue left unexplored was whether there were differences in RTP-beam calibration values between CST-5 and CST-7 Phase-2.)

6.2 Valid times

The valid times for 138°-R beam used in the reprocessing are indicated as dashed vertical lines in Fig. 11 for the SL-term curve. Fig. 14 shows the reprocessed RL curves for both signals for just these valid times. Fig. 12 shows the valid times—bounded by the chain-dotted vertical lines—used in the original processing. These differences are due to the different criteria used as to what is "valid": in the original processing, all times corresponding to bottom ensonification as long as a +3 SNR was maintained; in the reprocessing, a further restriction was applied, namely that only times where the bottom intersected with ±3 dB of the source beam pattern's MRA. It is recommended that the times be restricted to those where the source-beam pattern is known with some confidence.

6.3 Finite pulse-length and receiver-resolution adjustments

The reverberation decay rate was sufficiently small that these corrections (Henyey *et al.* 1996, Gauss 1996) were less than 0.25 dB and thus not a driver for the Run-1B data. (These are included in the newly-computed BSS's.)

6.4 SL

Because the two signals were at different frequencies (as were those in the shallow-water data), it is very important to examine the SLs applied in the original processing, and the impact of using the new mean SL-vs.-frequency curve derived earlier (Fig. 5). It should be noted that the SLs presented in Table 3 are the SLs for the *full 20-element array assuming* uniform *shading*—the Hamming and finite beamwidth of the source array are accounted for in the area and "dB-down" terms.

[7] We have some confidence that our calibration is accurate as we have run CST SUS data through the reprocessing stream and derived surface-scatter strengths. These have been shown to be consistent with perturbation theory at low wind speeds and frequencies (Ogden and Erskine 1994).

Original processing

Some inconsistencies arise here as to the intended and actual SLs used. It was stated that the SL at 936 Hz was 2.8 dB less than the (peak) SL at 880 Hz (Reilly, personal communication 1995), and that the representative SL curve from Dubord *et al.* (1990)—for the source with serial number 224—was used (Reilly, personal communication 1996). The latter suggests the SL at 936 Hz to be ~1.2 less than the SL at 880 Hz—see Fig. 4. However, **in either case, it appears that something close to the reverse was implemented in deriving the published results**, namely the array SL used at 936 Hz was 2.5 dB *greater* than that used at 880 Hz—see the headers of the "DP_56.DAT" files used in the two runs (Fig. 9), which states that the uniform SL used for the 1-s CW processing was 223.5 dB, while the SL used for that of the 0.25-s CW was 226.0 dB. **It is suggested that this is the major source of the observed PLD**. Note this is consistent with the basically grazing-angle independence of the phenomenon.

Reprocessing

As stated earlier, the source-level–vs.–frequency curve was determined to need modification. These newly derived values are the ones listed in Table 3 under reprocessing. Note the relative SLs between 880 and 936 Hz (~0.9 dB) basically match the relative SLs of the source with serial number 224 (~1.2 dB), i.e. (one of) the "intended SLs". (At each of these frequencies, there is still an absolute difference of 0.7 dB between the newly-derived and *these* intended SLs, reflecting mainly the Seneca-Lake, full-array vs. single-element calibration differences.)

The effects of using different sets of SLs for the two signals will be shown later when BSS curves are derived.

6.5 TL

In both processing methods, the two time-dependent, transmission loss terms are calculated by ray-based propagation codes, and depend primarily on the source-receiver geometry and the SSP.

6.6 A

A is the area returning energy to the receiver over any specified pulse length T. It is a time-dependent (range-dependent) quantity that depends on the signal characteristics (e.g., signal duration [CW] and bandwidth [HFM]); source and receiver beam patterns, tilts, and geometry; and sound speed at the bottom:

$$A \approx \Phi c T/2 \, .$$

This is a simplified version of what is actually calculated (which includes 3-D source and receiver beam patterns, bistatic geometries, etc.). A couple of notes:

- **Φ**. Here, the reductions in SL (or "dB down") due to the Hamming weighting (≥5.35 dB) on transmission *and* for being off the beams' MRAs are applied. Also accounted for here is the increase in area due to the Hamming receiver weighting (a factor of ~1.4, or ~1.5 dB).
- **cT**. For CW signals, the area scales by the pulse length, T, so that, for example, the area term for a 1-s signal is ~6.0 dB greater than that of a 0.25-s signal. For broadband signals (of bandwidth W), T is effectively replaced by 1/W, the signal's range resolution.

For the reprocessed data, one should combine the "A" and "dB-down" terms listed in the time-interpolation print files (and in Table 3) when computing BSS.

6.7 WA

The original processing combines the TL and A terms into a time-series representation of the (modeled) weighted area,

$$WA \equiv 10\log A - TL_{out} - TL_{back}$$

The WAs vs. time for the two processing programs agree very well (within a dB)—e.g., see Table 3.

6.8 SL + WA

Fig. 12 displays not only the originally-processed RL vs. time for the two CW signals, but SL+WA as well. To retrieve these values, the printed WAs and SLs from DP_56.DAT and SA_56.INP/OUT files were used—they agree well with (blow-ups of) the curves in this figure, i.e.:

$$SL_{0.25-s} + WA_{0.25-s} \approx SL_{1.0-s} + WA_{1.0-s} - 3 \ .$$

However, we also know for a given time, that $WA_{0.25-s} + 6 \approx WA_{1.0-s}$. Hence, upon substitution into the previous equation, we have:

$$SL_{0.25-s} \approx SL_{1.0-s} + 3 \ ,$$

or

$$SL_{936Hz} \approx SL_{880Hz} + 3 \ .$$

However, in actuality, $SL_{880Hz} \approx SL_{936Hz} + 1$, so that **there is approximately a 4-dB error[8] in the relative SLs used in deriving the reported CST-5 HF Run 1B BSS's.**

For completeness, Figs. 13a and b display the equivalent curves for the reprocessed 1- and 0.25-s CWs, respectively. (As the WAs for the two methods roughly agree and the SLs do not, the SL+WAs naturally disagree basically as much as the SLs disagree—see Table 3.)

6.9 BSS

BSS depends on combining all of the above via the sonar equation and correctly converting BSS as a function of time to BSS as a function of mean grazing angle.[9] An assumed 3-dB multipath—surface-reflected path—contribution was taken out at this stage for both processing methods.

Figs. 15 and 16 show the *reprocessed* BSS's presented with 3 sets of SLs. Fig. 15a uses the SLs in the original DP_56.DAT files. These generally reproduce Fig. 1a *modulo ~6–7 dB increases due to the revised RLs* and, as stated above, restrict the range of valid angles, so that the flatness of the BSS dependence on grazing angle is no longer so assured. Fig. 15b uses the "originally intended" SLs (Reilly, personal communication 1995). Doing so, shows no PLD. Fig. 16 uses the newly-derived SLs ($\approx$ the other intended SLs that were based on the S/N-224 source). Here, while the 1-s–CW BSS is ~1–2 dB greater than the 0.25-s–CW BSS, the general conclusion would be again, no basis for a PLD.

The sensitivity of the results was studied:

- Subaperture Length. The effect of subaperture length is seen in Fig. 17a, which uses the same input as Fig. 16, except a subaperture of 34 phones was used to form 35 beams (as opposed to 64 phones used to form 65 beams). General agreement between the two is seen. (The original processing used 103 phones to form 65 beams, which overlapped at their 2-dB–down points.)

[8] A 6-dB error assuming the "originally-intended" SLs.

[9] Curious aside: there were differences of ~ 0.15-0.2 s (for both signals) between the original processing and reprocessing as to what times corresponded to what grazing angles—see Figs. 9 and 10.

- Source Tilt. The effect of source tilt can be seen by comparing Fig. 17a (4-deg tilt) with Fig. 17b (3-deg tilt). Again, there is general agreement in level between the two. However, the 0.25-s CW results display some sensitivity of grazing-angle behavior to source tilt. This suggests that in general whether BSS is described as Lambertian or not could reflect the choice of source tilt, a parameter that is not always known to within a degree.[10]

  Independent of source-tilt considerations, BSS at low frequencies can often be driven not by scattering from the water-sediment interface (as assumed in the data processing) but from within the subbottom (Holland *et al.* 1996a). It is believed that these data are so driven (Holland *et al.* 1996b). In such a case, the "measured" bottom scatter can contain artifacts which are a function of sediment propagation and scattering as well as the experimental geometry. (In particular, plane-wave models—including Lambert's Law—may be inappropriate when subbottom scattering dominates.) For these data then, one should use a geoacoustic model capable of predicting and interpreting the artifacts associated with subbottom scattering. Such an approach applied to the CST-5 Run 1B BSS's is detailed in Holland *et al.* (1996b).

- Other Look Directions. Figs. 18a and b show the reported BSS's for other receiver beams for the 1-s and 0.25-s CWs, respectively. Fig. 19 shows the corresponding plots for the reprocessed data using the newly-derived SLs. The same general ~5-dB spreads are seen; again, both the absolute levels and the grazing-angle coverage differ between the reported and the reprocessed results.[11] The increases in the reported BSS's with *decreasing* grazing angle (especially evident in the 1-s data) are primarily due to the inclusion of extra times (15 to 20 s after transmit) as valid, coupled with beam-dependent source-tilt and timing effects. A more direct comparison of the reprocessed 0.25-s and 1.0-s BSS's is presented in Fig. 20 for four different look directions.

- Timing. The effect on BSS of errors in converting time to grazing angle for the CW signals is shown in Fig. 21. Here, to match the original processing, rather than properly referencing time relative to the center of the pulse of duration T, time shifts of $-T$ have been incorporated. (Thus, a bigger effect for a 1-s CW than for a 0.25-s CW.) Comparison with the corresponding curves of Fig. 20 shows that the main differences are for the 1-s CWs: ~1-deg shifts in grazing angle which translate into ~2-dB changes in level in Fig. 1a. Hence, *timing errors were the other notable contributor to the reported differences between the 1.0- and 0.25-s CW BSS's.*

6.10 Comparison with HFM results from Run 1B

As an additional check, BSS's were derived from the HFM data during the reprocessing. The HFM data results presented in Fig. 22 agree in level with the 138.6°-R CW data results presented in Fig. 16, and again show do not demonstrate a PLD. (In fact, the 1-s HFM BSS's are a couple of dB higher than those of the 2-s HFM, whereas the 1-s CW BSS's are a couple of dB higher than those derived from the 0.25-s CWs. In each case, the lower frequency BSS's are higher.)

[10] An *ad hoc* method to "back out" the source tilt is to overlay the RL curve with a family of SL+WA curves, parameterized by source tilt. Doing so in our case, a source tilt of 3.5° was found to produce the best match.

[11] The *apparent* beam dependence of the BSS at higher grazing angles is *not* due to any actual azimuthal dependence of the environment but due to the principal scattering mechanism (the sediment volume) being different from that assumed in the data processing (i.e. the water-sediment interface). For a general discussion, see Holland *et al.* (1996a).

6.11 Comparison with Run-2 SUS results

In addition to controlled waveform measurements, impulsive sources were used to collect bottom scattering data. These experiments used SUS charges attached to drag plates, so that the charges detonated (at depths of roughly 530 m) directly under the HFA, yielding a quasi-monostatic geometry. Despite using an omnidirectional source, low-grazing-angle bottom scattering strengths were obtained by using near-endfire beams, formed by an adaptive beamformer designed to suppress sidelobe interference from high-grazing-angle scatter (i.e. allowing "looking past" the fathometer returns, which had previously limited angle coverage to intermediate grazing angles) (Ogden and Erskine 1995).

SUS measurements were interleaved with the Run-1 controlled waveform measurements, with SUS Run 2 conducted immediately prior to Run 1B. For this SUS run, there is reason to believe that for the aft-most beam (160° R) there was little contamination by hybrid paths and that fathometer interference has been eliminated (Ogden, personal communication 1996). The HF BSS's for this beam—Fig. 23—show general agreement with the newly derived BSS's shown in Fig. 22, with the 1-s HFM results directly overlaying the 160°-R beam SUS results.

7. CST-5 RUN 44: IMPLICATIONS OF RUN-1B ANALYSIS

While the Run-44 data were not reprocessed, a simple analysis was performed to explore the possibility that a misapplication of SLs could be responsible for the PLD seen in Fig. 1b. To this end, (blow-ups of) the SL + WA curves from Reilly and Sundvik (1992), Fig. 24, were examined. The result is:

$$SL_{0.05-s} + WA_{0.05-s} \approx SL_{0.1-s} + WA_{0.1-s} + 3 \ .$$

However, we also know for a given time, that $WA_{0.05-s} + 3 \approx WA_{0.1-s}$. Hence, upon substitution into the previous equation, we have:

$$SL_{0.05-s} \approx SL_{0.1-s} + 6 \ ,$$

or

$$SL_{935Hz} \approx SL_{1004Hz} + 6 \ .$$

However, in actuality, $SL_{935Hz} \approx SL_{1004Hz} + 2$, so that the 0.05-s BSS's in Fig. 1b need to be raised $\approx$ 4 dB relative to the 0.1-s BSS's. **Doing so, the reported PLD disappears.** (Timing errors are unimportant here due to their short durations.)

8. CST-7 PHASE 3: IMPLICATIONS OF CST-5 RUN-44 ANALYSIS

As the CST-7 Phase 3 runs used the same HF waveforms as CST-5 Run 44, it appears the reason PLD was not prominently seen in the reported CST-7 Phase-3 results (e.g., in Run 17—Fig. 2b) was that the *intended* SLs did get used in deriving their BSS's. Given that the reported PLD differences in the CST-7 Phase-3 data results were at most a few dB (when present at all), it is concluded that there is no experimental evidence from these data that support a PLD phenomenon.

9. CONCLUSIONS AND RECOMMENDATIONS

9.1 Summary of results and conclusions

The results of this study have concluded there are two reasons for the reported pulse-length dependence of bottom scattering strengths. *First*, evaluation of the CST-5 Run-1B input parameters used in generating the reported 1-s, 880-Hz CW BSS's revealed an apparent use of a source level that was ~4 dB too low (relative at least to the 0.25-s, 936-Hz CWs). Making this adjustment raises the previously reported 0.25-s CW BSS's by ~4 dB. A similar adjustment (~4 dB) appears

to be required with the 0.1-s and 0.05-s CW data of CST-5 Run 44. *Second*, there was an additional ~2-dB difference between the 1-s and the 0.25-s CW Run-1B BSS's due to an error in how time was converted to grazing angle in the original processing. Hence, as the reported PLDs for other CST cases were at most a few dB (when present at all), **these corrections basically nullify the reported pulse-length dependence of bottom scattering strengths.** These effectively time-independent adjustments are consistent with the observed grazing-angle independence and help understand why the phenomenon was primarily observed only in the highest CST frequency band.

A secondary issue resolved is the large difference in the range of valid times (grazing angles) as calculated by the two processing methods. This was due to differences in source-beam-pattern assumptions. Restricting the range of valid times could obviate some of the "flatness" trend in grazing angle (*re* Lambert) reported for the deep-water, coherent-pulse BSS's. IT IS RECOMMENDED THAT THE TIMES BE RESTRICTED TO THOSE WHERE THE SOURCE-BEAM PATTERN IS KNOWN WITH SOME CONFIDENCE.

A beam-dependent sensitivity of the grazing-angle behavior of the CST-5 BSS's to the assumed source tilt of 4 deg was noted. Hence, in general, experimentalists should make some effort to acquire accurate knowledge of source and receiver geometries (and include error bars on their results that reflect the range to which their sonar-equation analysis parameters—such as source tilt—are known). Furthermore, in this particular case, the subbottom dominates the scattering process (and not the water-sediment interface as assumed in both the original and the reprocessing). In such cases where the subbottom dominates the scattering process, a geoacoustic model that accounts for subbottom propagation and scattering as well as the experimental geometry is required to predict and interpret the data results.

A still unresolved issue is why the reprocessed *absolute* Run-1B RLs were 5.5–7 dB higher in general than those of the originally reported RLs. There is no explanation for this at the moment. *If* there is a systematic calibration error, this could potentially affect the reported LF and MF BSS's as well.

These results are consistent with theoretical expectations of a pulse-length independence of scattering strengths (whenever the frequency dependence of the scattering strengths can be neglected). Further experimental evidence was presented showing that the bottom scattering strengths derived from coherent and incoherent source data were identical within measurement uncertainties. Other statistics can depend on the waveform, but the scattering strength cannot (Thorsos *et al.* 1996). (Waveform statistics will generally only be the same if the scattering process is Gaussian.)

9.2 Recommendations

Due to near-field effects, *apparent* PLD effects can be observed in acoustic field data: longer pulses and greater decay rates both can bias scattering strengths upward when estimated with the standard algorithm. However, straightforward formulas have been developed to correct for these biases—see the Appendix. It should be noted that these corrections do *not* require any knowledge of the subbottom or the system used to collect the data. To support prediction capabilities for active systems, procedures should be identified for realizing such corrections for *apparent* pulse-length dependent effects at the operational level, "automatically" if possible (maybe only in the next generation of a particular system). At a minimum, operators should become cognizant of the phenomena. Two such procedures include either:

> Simulating (apparent) pulse-length effects when generating model curves for prediction or comparison with data curves (e.g., running a "T-second" window over the predicted RL curve of an impulsive signal),

or

Correcting the data curves and then comparing them with model predictions of impulsive signals (e.g., to invert for bottom parameters).

10. ACKNOWLEDGMENTS

This work was prepared under the sponsorship of Mr. Charles I. Bohman of the Space and Naval Warfare Systems Command, PMW-182. Thanks to Lillian Fields, Planning Systems Inc., for reprocessing the data. Some of the work presented in this paper was supported by the Office of Naval Research (NRL *Active Acoustics* project UW-35-2-03).

11. REFERENCES

C.J. Dubord, W.L. Clay, W.L. Konrad and J. Monti (**1990**), "Calibration Procedures and Results for the FLOSS 90 Flextensional Vertical Array," NUSC Technical Memorandum No. 901011.

R.C. Gauss, J.M. Fialkowski and R.J. Soukup (**1993**), "Intermediate-Pulse Direct-Path Measurements of Surface Scattering in CST-7 Phase II," JHU/APL Technical Report STD-R-2258, "Critical Sea Test 7, Phase II - Principal Investigators' Results, Volume 1: Surface Scattering and Volume Scattering Measurements," ed. F. Erskine.

R.C. Gauss, P. M. Ogden, J.B. Chester and J.M. Fialkowski (**1995**), "Deriving scattering strengths from nonstationary time-series data: A comparison of low-frequency surface-backscattering strengths using both impulsive and coherent sources," J. Acoust. Soc. Am. **97** (5), Pt. 2, 3403 (A).

R.C. Gauss (**1996**), "Critical Sea Test Surface Interaction Overview," CST/LLFA-WP-EVA-45A, Space and Naval Warfare Systems Command, Arlington, VA.

R.C. Gauss, C.W. Holland, J.M. Fialkowski, and P. Neumann (**1996**), "Measurements and modeling of low-frequency bottom-scattering strengths from the Scotian Continental Rise," J. Acoust. Soc. Am., **100**, Pt. 2, 2797 (A).

F.S. Henyey, E.I. Thorsos and K.M. Nathwani (**1995**), "Scattering strength cannot depend on the length of a pulse," J. Acoust. Soc. Am. **98** (5), Pt. 2, 2986–2987 (A).

F.S. Henyey, K.M. Nathwani and E.I. Thorsos (**1996**), "Pulse Length/Type Independence of Scattering Strength for Bottom Scattering," APL/UW Technical Memorandum TM 5-96, Applied Physics Laboratory, University of Washington.

C.W. Holland, P.M. Ogden, M.T. Sundvik and R. Dicus (**1996a**), "Critical Sea Test Bottom Interaction Overview," CST/LLFA-WP-EVA-46, Space and Naval Warfare Systems Command, Arlington, VA.

C.W. Holland and P. Neumann (**1996b**), "Sub-bottom Scattering and Loss: Analysis of a CST data set," CST/LLFA-WP-EVA-1, Space and Naval Warfare Systems Command, Arlington, VA.

J.E. Moe and D.R. Jackson (**1994**), "First-order perturbation solution for rough surface scattering cross section including the effects of gradients," J. Acoust. Soc. Am. **96** (3), 1748–1754.

P.M. Ogden and F.T. Erskine (**1993**), "Low-Frequency Bottom Backscattering Strengths Measured using SUS Charges," Proc. I.O.A., **15**, Part 2, 271–278.

P.M. Ogden and F.T. Erskine (**1994**), "Surface scattering measurements using broadband explosive charges in the Critical Sea Test experiments," J. Acoust. Soc. Am. **95** (2), 746–761.

P.M. Ogden and F.T. Erskine (**1995**), "Bottom backscattering strengths at low grazing angles using adaptive beamforming," J. Acoust. Soc. Am. **97** (5), Pt. 2, 3385 (A).

P.M. Ogden and R.C. Gauss (**1996**), "Comparison of direct-path surface scattering results obtained using controlled waveforms and SUS charges," CST/LLFA-WP-EVA-30A, Space and Naval Warfare Systems Command, Arlington, VA.

S.M. Reilly and M.T. Sundvik (**1992**), "CST-5 Direct Path, Active Waveform Bottom Reverberation Analysis," Tracor Doc. No. T92-95-1013-U.

S.M. Reilly and S. Craig (**1993**), "Bottom Scattering Measurements," Chapter 10 in JHU/APL Technical Report STD-R-2260, "Critical Sea Test 7, Phase 3 - Principal Investigators' Results: Shallow-Water LFA Systems Measurements in the Northeast Pacific Ocean; Volume 3 of 3: Environmental, Scattering, and Propagation Measurements," ed. J.B. Edgerton.

S.M. Reilly (**1994**), "Bottom Reverberation Measurements in the Nile Fan using an Echo Repeater," Tracor Doc. No. T94-95-1011-U.

S.M. Reilly, R.J. Christian, J.B. Chester and M.J. Vaccaro, (**1995a**) "Pulse Length Dependence in the CST Bottom Reverberation Measurements," Tracor Doc. No. T95-95-1002-U.

S.M. Reilly, R.J. Christian, J.B. Chester and M.J. Vaccaro, (**1995b**), "Pulse length dependence in CST bottom reverberation measurements," J. Acoust. Soc. Am. **97** (5), Pt. 2, 3385–3386 (A).

E.I. Thorsos, D.B. Percival, and K.M. Bader (**1996**), "Modeling low-frequency surface scatter intensity statistics," J. Acoust. Soc. Am., **100**, Pt. 2, 2799 (A).

M.J. Vaccaro, P.M. Ogden, R.C. Gauss, J.B. Chester, S.M. Reilly, C.W. Holland, B. Gardner, C.S. Hayek, M.D. Mandelberg, C.H. Thompson, M. Huster, F.S. Henyey, J. Pupek, and C.R. Burrus (**1996**), "Critical Sea Test Program: Experimental Methods for Environmental Acoustics," SPAWAR CST/LLFA-WP-EVA-42, Space and Naval Warfare Systems Command, Arlington, VA.

CST	Run	Descrip	Band	Transmission						
				Waveform	f_c (Hz)	T (sec)	W (Hz)	SL_{elem} (dB) Intended	Used	Revised
5	1B	Deep	**HF**	CW	880	1.0	< 1 >	203.5	197.5	202.8
				CW	936	0.25	< 4 >	202.3 or 200.7	200.0	201.9
				HFM	890	1.0	20			202.8
				HFM	950	2.0	100			201.4
5	44	Shallow	**HF**	CW	1004	0.10	< 10 >			199.8
				CW	935	0.05	< 20 >	202.3		201.9
7 P3		NS,C,SS	**HF**	CW	1004	0.10	< 10 >			199.8
		SS		CW	935	0.05	< 20 >	202.3		201.9
		NS,C,SS		HFM	935	0.25	70			201.9
		NS,C,SS		HFM	960	0.25	120			201.2
		NS,S,C,SS	MF	CW	380	0.05	< 20 >			204.2
		NS,S,C,SS		CW	412	0.10	< 10 >			206.2
		S,C,SS		HFM	380	0.25	70			205.7
		NS,S,C,SS	LF	CW	247	0.08	< 12.5 >			
		NS,S		HFM	250	0.25	60			
NS = North Shelf (Run 12–LF/MF/HF), S = Slope (13–LF/MF), C = Canyon (17–HF,21–LF/MF), SS = South Shelf (17–LF/MF/HF)										
8	C10		LF	CW		0.10	< 10 >			
				CW		0.25	< 4 >			
				HFM		0.25	66			
8	C13		**HF**	CW		0.10	< 10 >			
			LF	CW		0.10	< 10 >			
				CW		0.25	< 4 >			
				HFM		0.25	66			
8	C18		**HF**	CW		0.25	< 4 >			
			LF	CW		0.10	< 10 >			
				CW		0.25	< 4 >			

Table 1 – Summary of transmission parameters: selected CST-5 through CST-8 Runs. Mean individual element source levels (dB re 1 μPa @ 1 m) are shown. (Bandwidths for the CWs represent their 4-dB–down spreads about f_c.)

Run	Processing	Source					Receiver	Beamformer		S–R sep.	XBT
		Elements used	Steering (deg)	Tilt (deg)	Shading	Depth (m)	Depth (m)	No. of Beams	Phones used	(Hor. proj.) (m)	Cast
1B	Original	1–20	down 25	4	Hamming	130	138	64	22–124	880.08	1009
	Reprocessing	1–20	down 25	4	Hamming	130	138	65	22–85	880	1009

Table 2 – Summary of parameters used in original and reprocessing of the HF CST-5 data. The receiver beams had Hamming weighting. Ship speed assumed to be 2.9 kts.

CW Dur (s)	Time wrt xmit	Proc.	RL	Mean Gr Ang	2-way TL	A (dB)	dB down	WA = A + dB_{dn} - TL	Unif. SL	SL + WA	BSS RL - SL -WA -3.2
1.0	12.5	Original	80.5	17.0				-104.2	223.5	119.3	-42.0
		Reprocess	85.5	17.3	159.2	60.7	-5.9	-104.4	228.8	124.4	-42.1
	13.0	Original	79.8	16.1				-104.7	223.5	118.8	-42.2
		Reprocess	83.8	16.4	159.8	60.8	-6.0	-105.0	228.8	123.8	-43.2
	13.5	Original	78.3	15.2				-104.6	223.5	118.9	-43.8
		Reprocess	82.6	15.5	160.5	61.0	-6.2	-105.7	228.8	123.1	-43.7
	14.0	Original	75.8	14.4				-106.6	223.5	116.9	-44.3
		Reprocess	82.1	14.7	161.1	61.1	-6.6	-106.6	228.8	122.2	-43.3
	14.5	Original	74.9	13.6				-108.2	223.5	115.3	-43.6
		Reprocess	82.4	13.9	161.7	61.2	-7.1	-107.6	228.8	121.2	-42.0
	15.0	Original	74.8	13.0				-108.9	223.5	114.6	-43.0
		Reprocess	81.1	13.3	162.2	61.3	-7.6	-108.5	228.8	120.3	-42.4
											RL - SL -WA -3.1
0.25	12.5	Original	69.7	17.0				-109.3	226.0	116.7	-50.1
		Reprocess	77.4	17.3	159.1	54.4	-5.9	-110.6	227.9	117.3	-43.0
	13.0	Original	66.9	16.1				-110.3	226.0	115.7	-51.9
		Reprocess	74.7	16.4	159.8	54.5	-6.0	-111.3	227.9	116.6	-45.0
	13.5	Original	66.9	15.2				-111.0	226.0	115.0	-51.2
		Reprocess	72.8	15.6	160.4	54.7	-6.2	-111.9	227.9	116.0	-46.3
	14.0	Original	64.2	14.4				-113.1	226.0	112.9	-51.8
		Reprocess	73.6	14.8	161.0	54.8	-6.7	-112.9	227.9	115.0	-44.5
	14.5	Original	63.2	13.6				-113.1	226.0	112.9	-52.8
		Reprocess	71.1	14.0	161.6	54.9	-7.2	-113.9	227.9	114.0	-46.0
	15.0	Original	62.7	12.8				-114.8	226.0	111.2	-51.6
		Reprocess	68.2	13.3	162.2	55.0	-7.8	-115.0	227.9	112.9	-47.8

Table 3 – The sonar equation term-by-term for the original processing and the re-processing. The BSS values—here indexed to the time (with respect to start of transmission) and *not* to the grazing angle—are only for processing-comparison purposes.

APPENDIX: NONSTATIONARITY CORRECTION FORMULA

A by-product of the CST direct-path waveform scattering strength analyses was a new understanding (and procedure) for correcting for near-field effects in direct-path measurements when using non-impulsive signals (Gauss *et al.* 1995; Henyey *et al.* 1995, 1996). Longer pulses and greater decay rates can both bias calculations towards earlier times where the scattering strength and grazing angle are higher and transmission loss is lower. Exploiting the fact that the reverberation level as a function of time generally obeys (locally) a power law—and assuming the timing is with respect to the center of the pulse—a careful (but straightforward) analysis can correct for these *apparent* pulse-length-dependent effects:

$$\Delta RL(t)\ (dB) = -10\log\left[\frac{10^{\left(1+\frac{b(t)T_S}{20}\right)} - 10^{\left(1-\frac{b(t)T_S}{20}\right)}}{b(t)T_S \ln 10}\right] - 10\log\left[\frac{10^{\left(1+\frac{b(t)T_P}{20}\right)} - 10^{\left(1-\frac{b(t)T_P}{20}\right)}}{b(t)T_P \ln 10}\right],$$

where $b(t)$ is the local slope of the reverberation decay curve $RL(t)$ in dB/s, T_S = pulse duration and T_P = processing resolution. These corrections are to be added to the $RL(t)$ curves (i.e. $RL_{true}(t) = RL_{observed}(t) + \Delta RL(t)$) *prior* to sonar-equation analysis. Generally, for a CW, $T_S = T_P$ = pulse duration, and for a broadband waveform (matched filter output), $T_S = T_P$ = 1./signal_bandwidth. Hence, the corrections are mainly important in CW analysis. (For an impulsive signal using a T_P-s processing window, there is just a $10log$ correction.) Fig. 25 presents ΔRL-vs.-bT curves, with examples of the magnitude of the corrections for CWs given in Table 4:

Near-field $RL(t)$ Corrections for CWs

Signal Duration (s)	Reverberation Decay Rate		
	5 dB/s	10 dB/s	15 dB/s
0.05	0	0	−0.01
0.25	−0.03	−0.12	−0.27
0.5	−0.12	−0.47	−1.05
1.0	−0.47	−1.84	−3.95
1.5	−1.1	−3.95	−8.16
2.0	−1.84	−6.65	−13.20
2.5	−2.81	−9.77	−18.77

Table 4 – Example near-field corrections for CW signals. Assumes processing window is matched to the signal duration ($T_S = T_P$).

Applying such corrections, excellent agreement was obtained between SUS and waveform (CW, LFM) surface-scattering results for signal durations between 0.05 and 2.4 s (Gauss *et al.* 1995, Ogden and Gauss 1996). (Analogous corrections are required for spectral spreading—see Gauss, Fialkowski and Soukup 1993.)

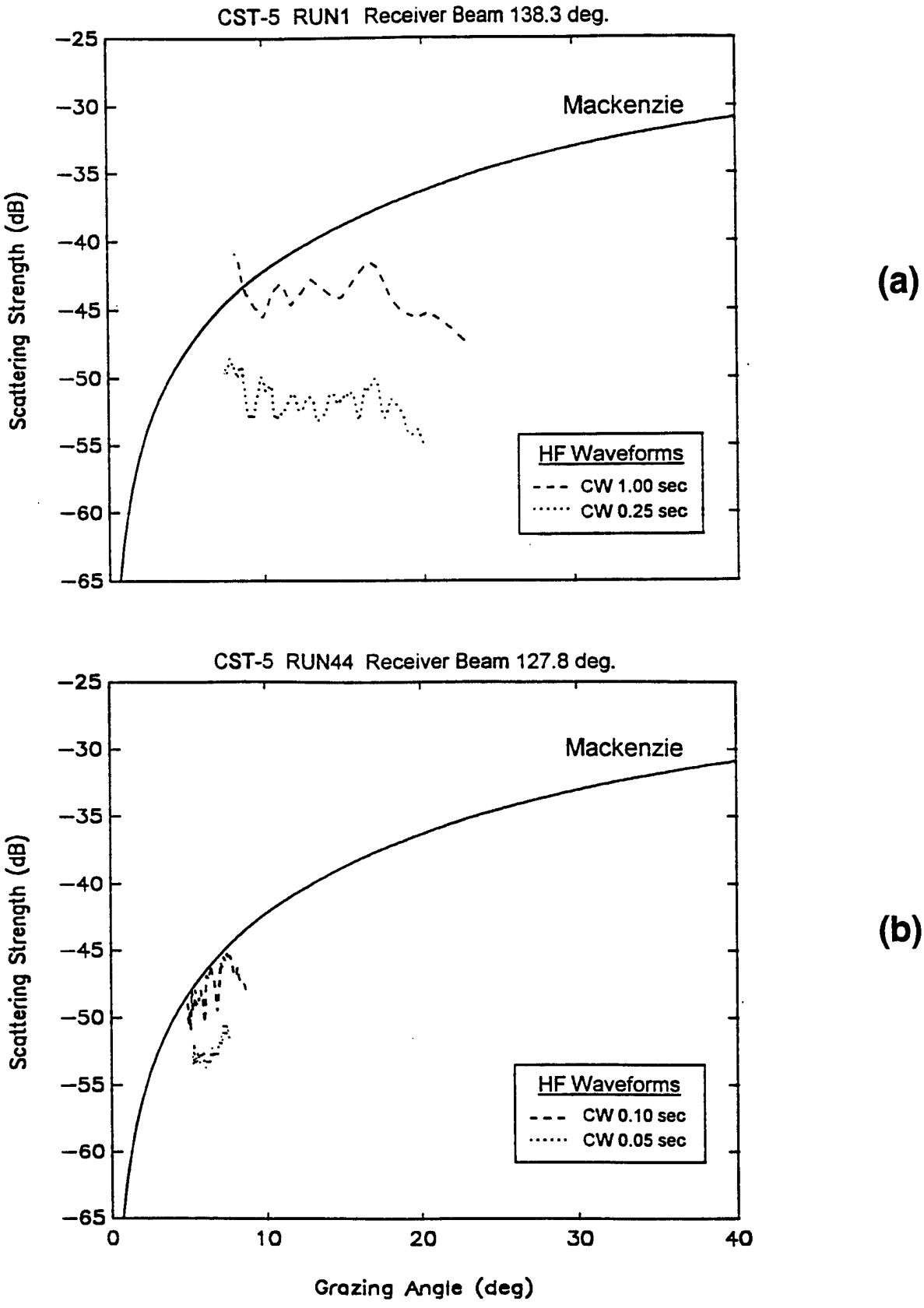

Fig. 1 – Previously published CST-5 **HF** Bottom Scattering Strengths: (a) Run 1B (deep water) (b) Run 44 (shallow water). (From Reilly *et al.* 1995a.)

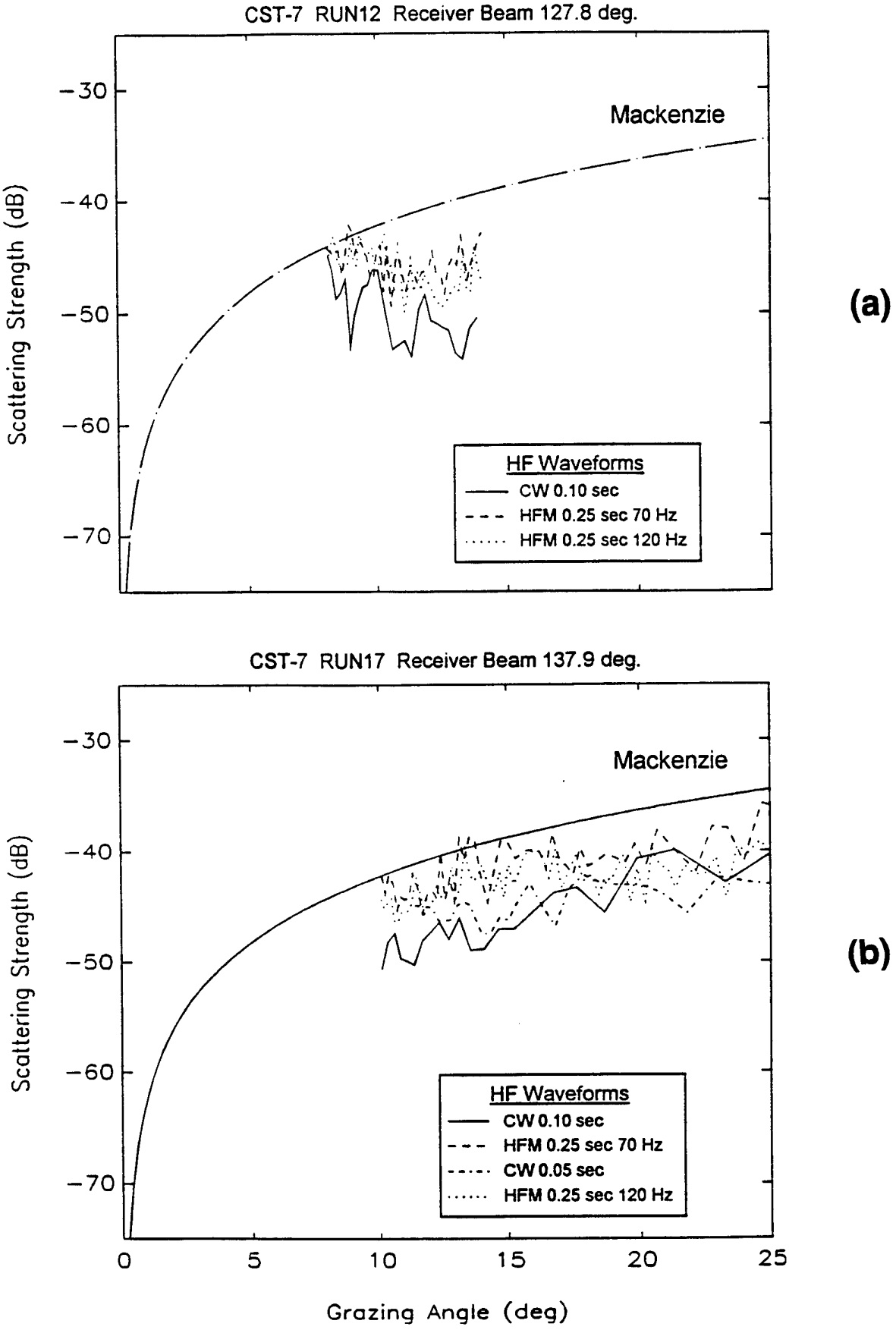

Fig. 2 – Previously published CST-7 Phase-3 **HF** Bottom Scattering Strengths: (a) Run 12 (shallow water—north shelf) (b) Run 17 (shallow water—south shelf). (From Reilly *et al.* 1995a.)

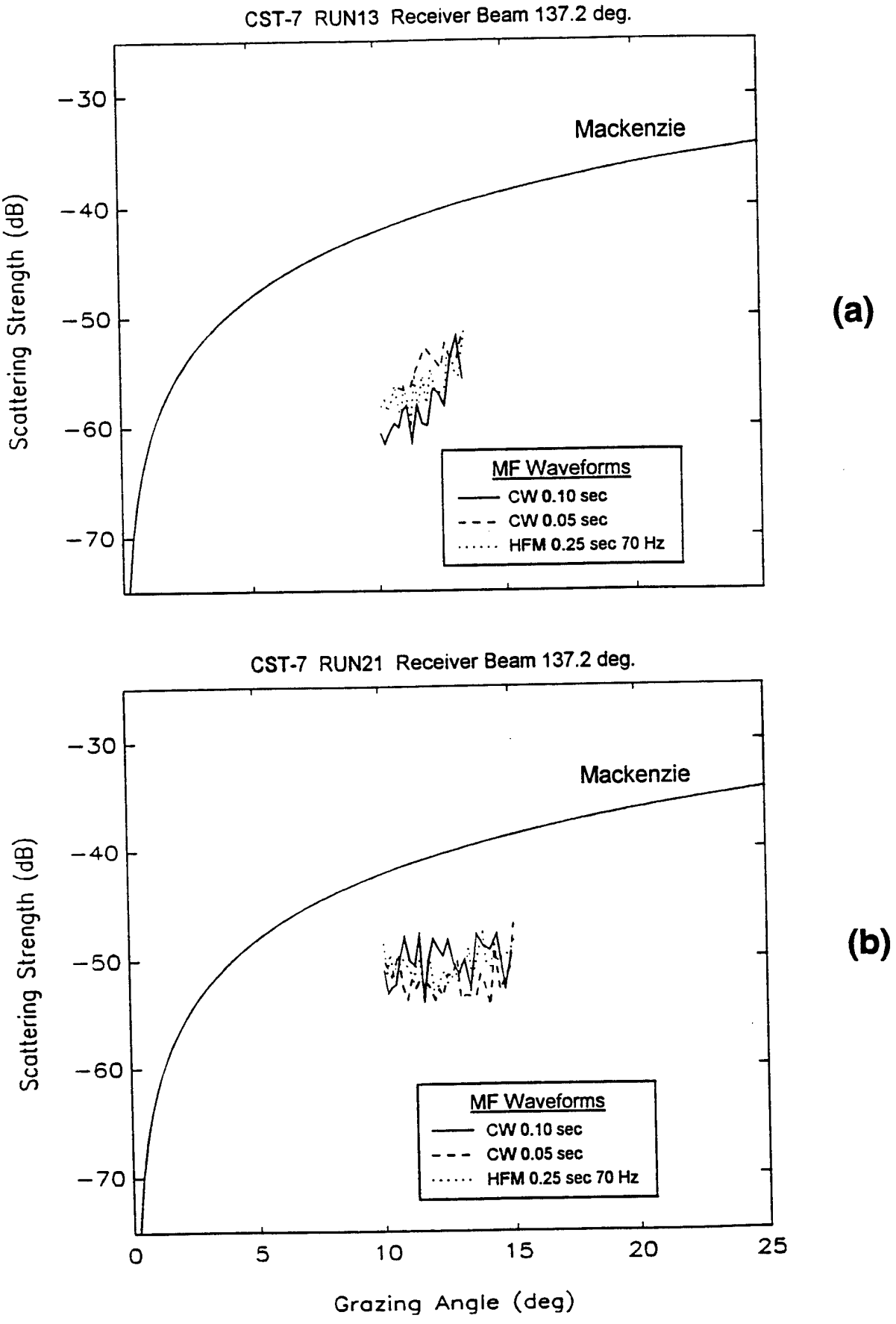

Fig. 3 – Previously published CST-7 Phase-3 **MF** Bottom Scattering Strengths: (a) Run 13 (shallow water—slope) (b) Run 21 (shallow water—canyon). (From Reilly *et al.* 1995a.)

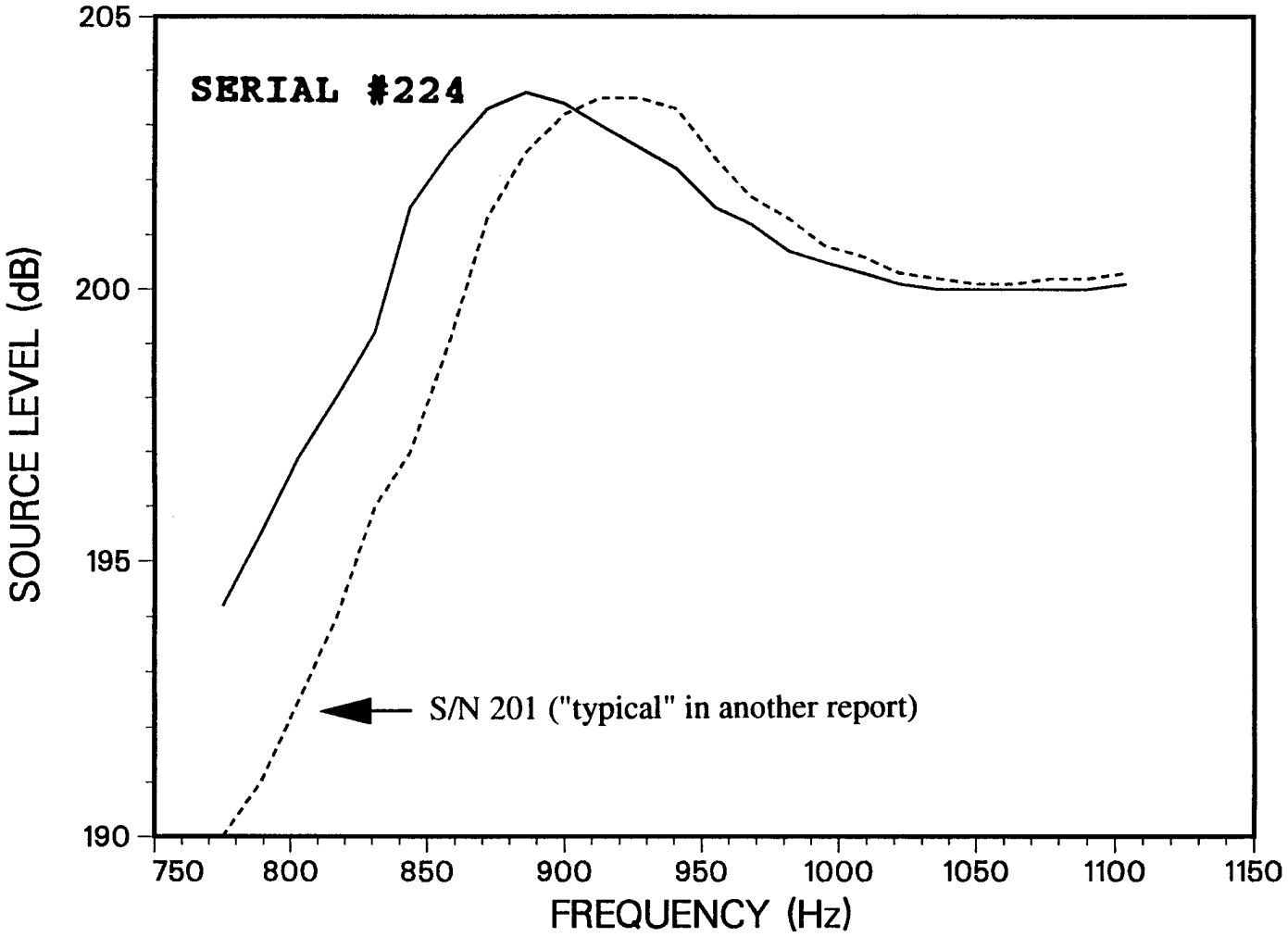

Fig. 4 – HF single-element source level vs. frequency curves: previously-assumed, "representative" curves. The solid curve was used in deriving the previously-published HF BSS's. (Derived from Dubord *et al.* 1990.)

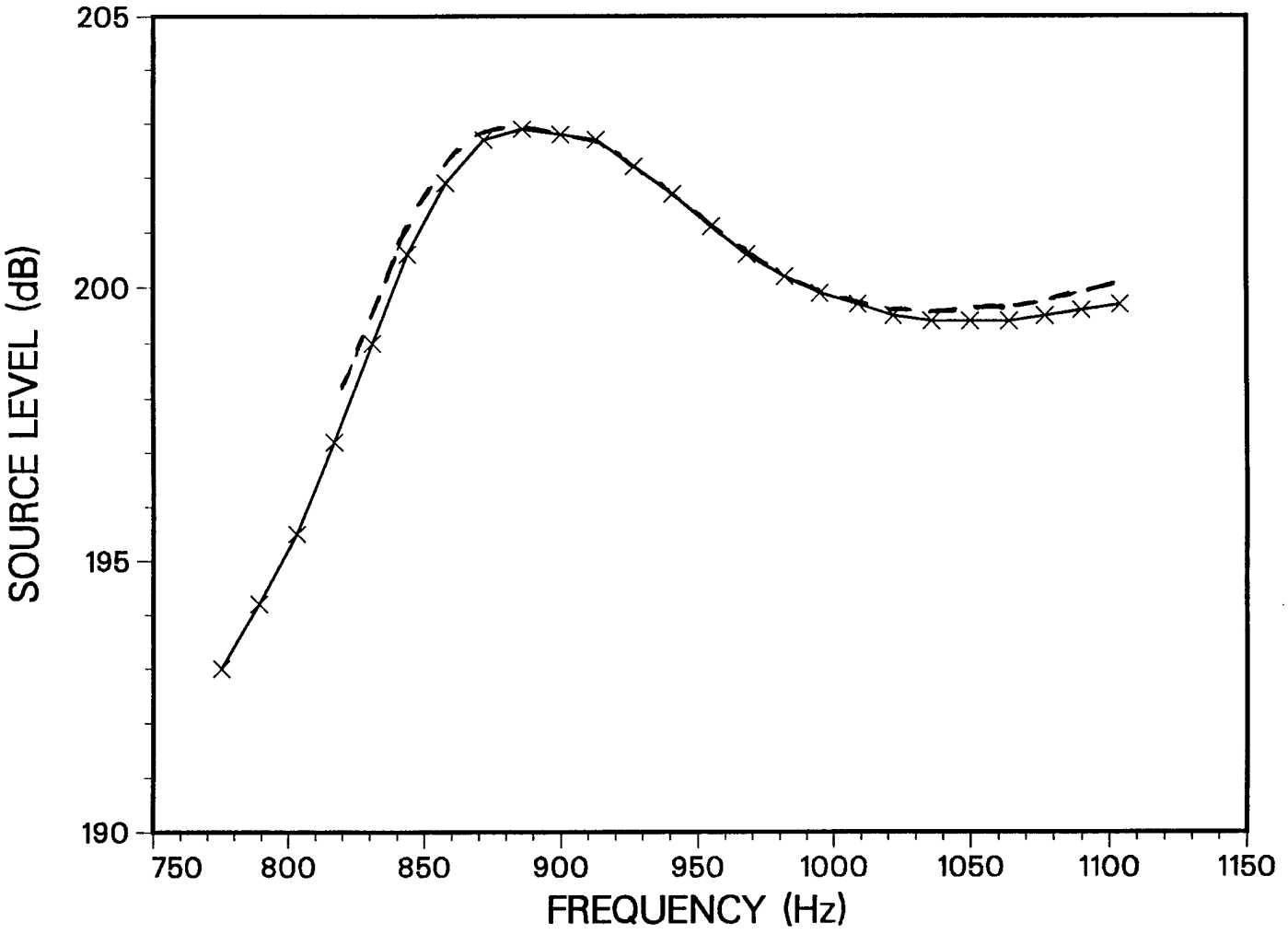

Fig. 5 – HF single-element source level vs. frequency: the solid curve represents the (linear) average of individual element responses collected during a Seneca-Lake calibration experiment; and the dashed curve measured data fitted to the peak of the solid curve. The solid curve includes a subtraction of 0.8 dB from the average to reflect the degradation measured at Seneca Lake when using an array of N elements compared to the single-element levels + $20 \log N$.

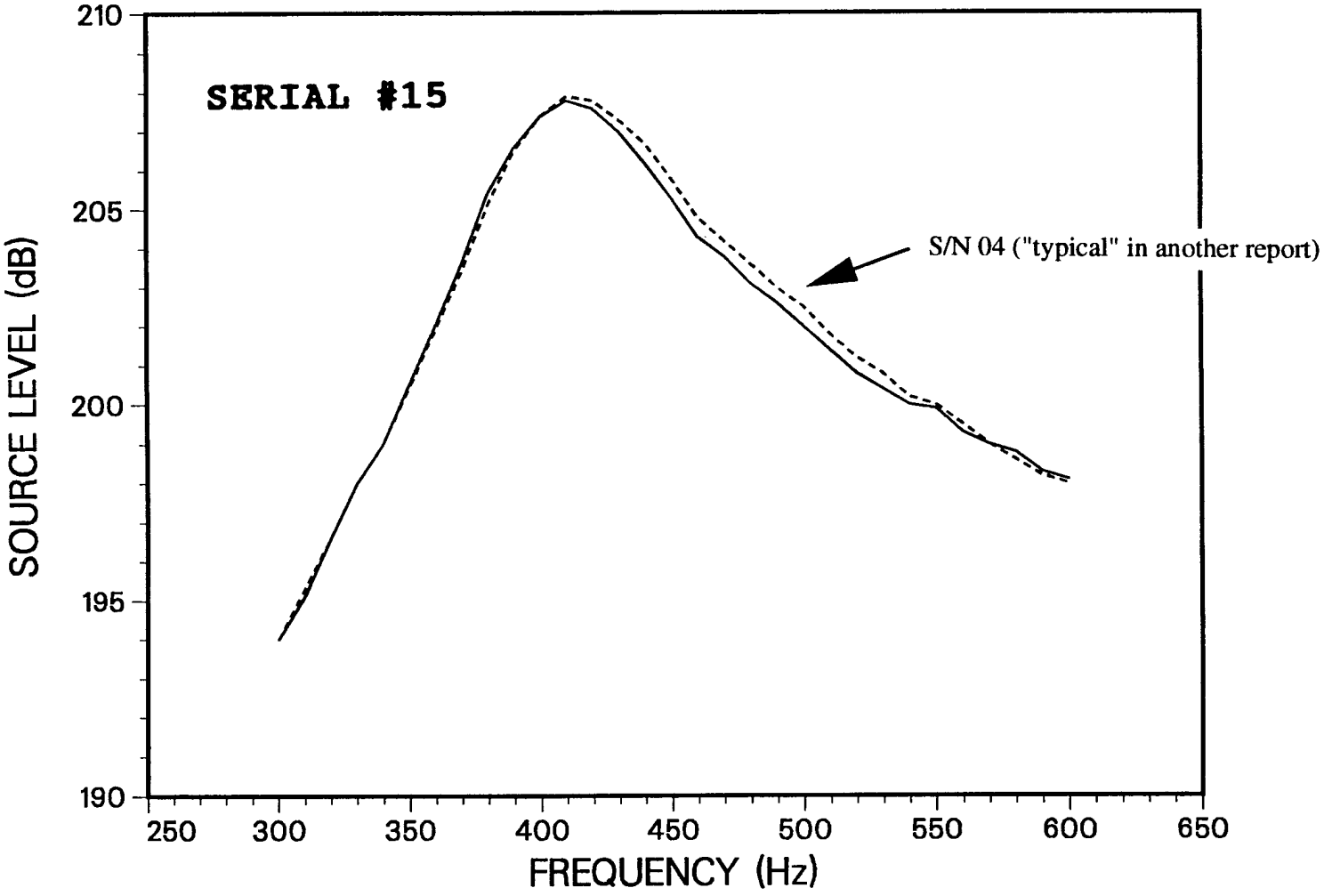

Fig. 6 – MF single-element source level vs. frequency curves: previously-assumed, "representative" curves. The solid curve was used in deriving the previously-published MF BSS's. (Derived from Dubord *et al.* 1990.)

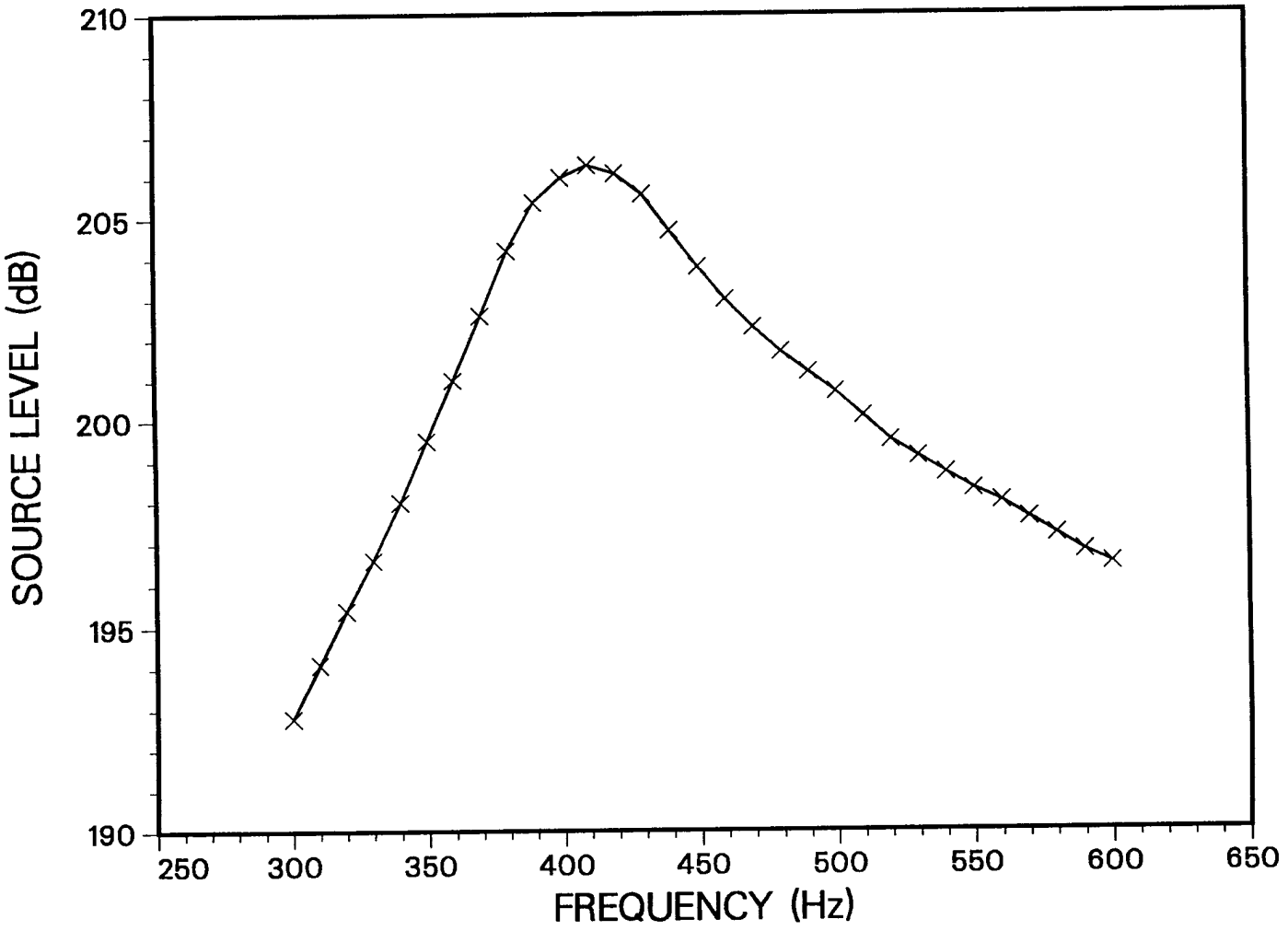

Fig. 7 – MF single-element source level vs. frequency: the curve represents the (linear) average of individual element responses collected during a Seneca-Lake calibration experiment. The curve includes a subtraction of 1.6 dB from the average to reflect the degradation measured at Seneca Lake when using an array of N elements compared to the single-element levels + $20 \log N$.

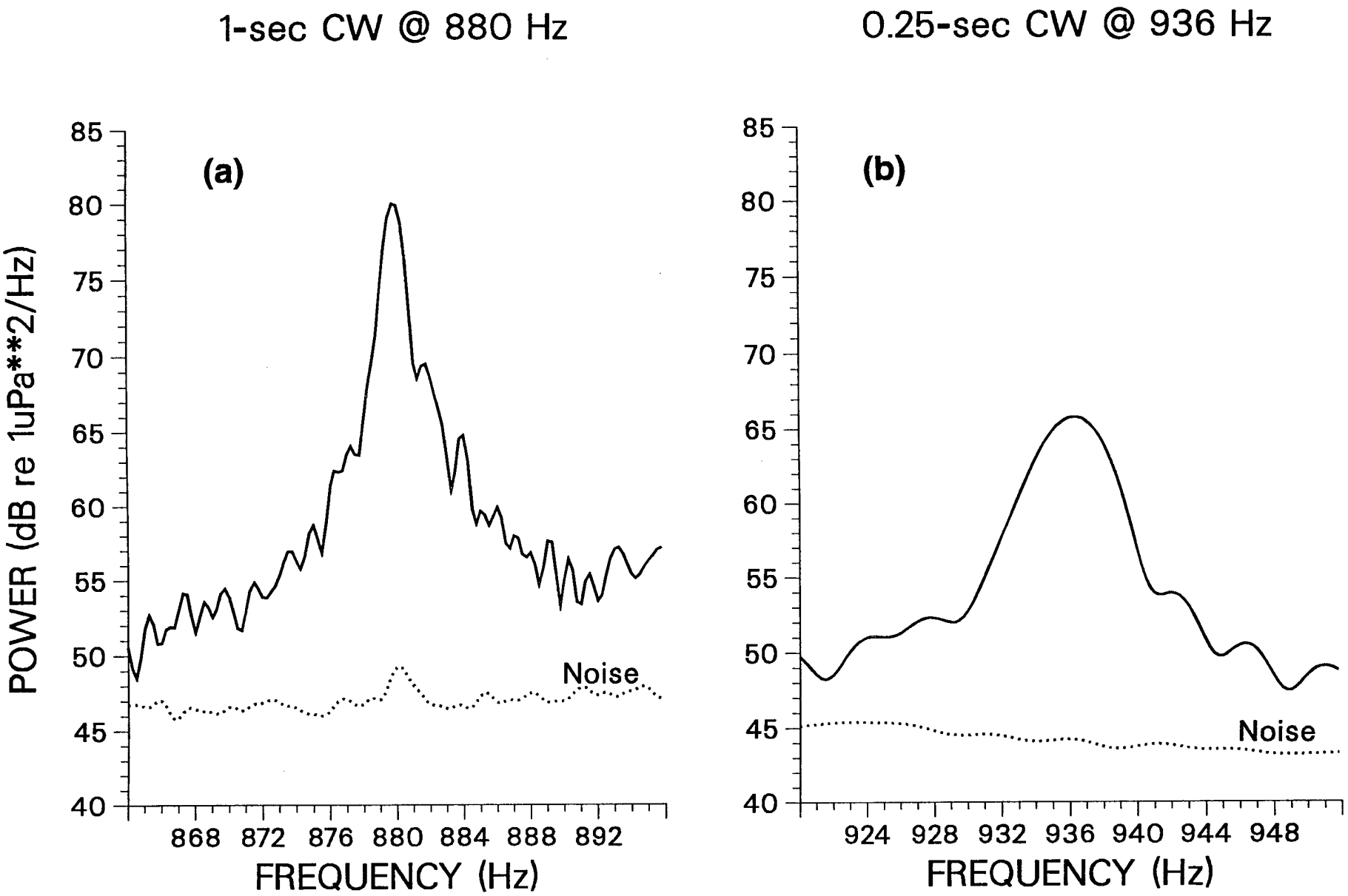

Fig. 8 – Representative CST-5 Run 1B spectra for the (a) 1-s, 880-Hz and (b) 0.25-s 936-Hz CWs at times corresponding to valid bottom backscatter (solid curves) and to background returns (dashed curves).

CST-5 Run 1B NAS Parameter Listing

CST NUMBER = 5
RUN NUMBER = 1
SEGMENT LETTER = H
JULIAN DAY = 161
BACKSCATTER TARGET = BOTTOM
LOCATION DESCRIPTION = IONIAN BASIN
INITIAL PING TIME = 02:15:04.28
START TIME SERIES = 0.58
STOP TIME SERIES = 20.58
ENSEMBLE AVERAGES = 12
PING REPETITION RATE = 120.
BOTTOM DEPTH = 11174. FT
TRANSMIT WAVETRAIN = WTBS04
SOURCE DEPTH = 426. FT
SOURCE WEIGHTING = HAMMING
SOURCE TILT = 4.0
SOURCE STEERING ANGLE = -25.0
SOURCE/RECEIVER SEPARATION = 0.8808
RECEIVER TYPE = HFAVH
RECEIVER DEPTH = 452. FT
RECEIVER WEIGHTING = HAMMING
BEAMFORMED PHONE START = 22
CONSECUTIVE CHANNELS BEAMFORMED = 108 [Error: Must mean 103]
BEAM SPACING FILE = BEAM$:COS64.DAT
BEAMFORMER SCALE FACTOR = 21380.
RTP INPUT SAMPLE RATE = 4096
REAL OUTPUT SAMPLE RATE = 512
RV1 SPEED (KTS) = 2.9
RV1 HEADING = 303.
RV1 COMEX LOCATION = 36.2733 N 17.1698 E
RV1 FINEX LOCATION = 36. N 17. E
ENVELOPE OFFSET = 128
ENVELOPE WINDOW = 512

1-s CW

CST NUMBER = 5
RUN NUMBER = 1
SEGMENT LETTER = I
JULIAN DAY = 161
BACKSCATTER TARGET = BOTTOM
LOCATION DESCRIPTION = IONIAN BASIN
INITIAL PING TIME = 02:17:06.09
START TIME SERIES = 7.58
STOP TIME SERIES = 27.58
ENSEMBLE AVERAGES = 19
PING REPETITION RATE = 120.
BOTTOM DEPTH = 11174. FT
TRANSMIT WAVETRAIN = WTBS26
SOURCE DEPTH = 426. FT
SOURCE WEIGHTING = HAMMING
SOURCE TILT = 4.
SOURCE STEERING ANGLE = -25.
SOURCE/RECEIVER SEPARATION = 0.8808
RECEIVER TYPE = HFAVH
RECEIVER DEPTH = 452. FT
RECEIVER WEIGHTING = HAMMING
BEAMFORMED PHONE START = 22
CONSECUTIVE CHANNELS BEAMFORMED = 103
BEAM SPACING FILE = BEAM$:COS64.DAT
BEAMFORMER SCALE FACTOR = 21380.
RTP INPUT SAMPLE RATE = 4096
REAL OUTPUT SAMPLE RATE = 512
RV1 SPEED (KTS) = 2.9
RV1 HEADING = 303.
RV1 COMEX LOCATION = 36.2733 N 17.1698 E
RV1 FINEX LOCATION = 36. N 17. E
ENVELOPE OFFSET = 32
ENVELOPE WINDOW = 128

0.25-s CW

Fig. 9 – For the original processing of CST-5 Run 1B data, printouts of various direct-path processing input parameters for both the 1-s and 0.25-s CWs.

CST-5 Run 1B *DP_56.DAT* File

CST RUN # 1H
DATA FILE: DP_56.DAT
NUMBER OF BEAMS = 64, NUMBER OF PINGS ENSEMBLE AVERAGED = 12
SOURCE LEVEL = 223.5 DB, START TIME = 161:02:15:04.28 ← **NOTE: SL value**
WEIGHTED AREA FILE: SA_56.OUT
VLA STEERING = -25.00, HLA STEERING = 138.25
NUMBER OF POINTS = 80 CENTER FREQUENCY = 880.

TIME	BACKSCAT	REVERB	S. GRAZE	I. GRAZE	BIANGLE	HLA BEAR	RVB-STD	RVB+STD
7.33000	-36.120	68.381	36.627	31.488	2.896	163.	-2.569	1.980
7.58000	-34.611	70.073	35.011	30.290	3.399	159.	-2.801	2.115
7.83000	-34.324	71.291	32.590	29.919	8.044	121.	-3.108	2.284
8.08000	-35.594	71.912	32.239	28.061	3.129	159.	-3.715	2.594
8.33000	-37.279	71.551	30.911	27.125	3.827	153.	-4.184	2.812
8.58000	-41.023	70.998	29.723	26.201	3.944	151.	-4.551	2.971
8.83000	-43.461	70.860	28.609	25.332	4.051	149.	-3.220	2.344
9.08000	-44.843	71.263	27.595	24.485	3.917	149.	-2.337	1.840
9.33000	-45.279	71.938	26.615	23.714	4.016	147.	-3.299	2.385
9.58000	-44.729	73.806	25.721	22.960	3.893	147.	-3.429	2.452
9.83000	-44.420	75.365	24.874	22.241	3.779	147.	-3.738	2.605
10.08000	-44.286	76.576	24.071	21.558	3.671	147.	-3.565	2.520
10.33000	-43.543	78.044	23.280	20.929	3.764	145.	-2.520	1.951
10.58000	-42.987	79.006	22.555	20.304	3.664	145.	-1.527	1.298
10.83000	-42.501	79.710	21.861	19.705	3.569	145.	-1.752	1.457
11.08000	-42.263	80.081	21.177	19.157	3.654	143.	-2.498	1.938
11.33000	-42.591	79.898	20.552	18.611	3.565	143.	-3.135	2.299
11.58000	-42.336	80.025	19.952	18.085	3.480	143.	-2.716	2.066
11.83000	-42.010	79.992	19.375	17.578	3.400	143.	-2.268	1.797
12.08000	-41.287	80.005	18.822	17.090	3.323	143.	-2.313	1.825
12.33000	-39.892	80.371	18.289	16.621	3.250	143.	-2.516	1.949
12.58000	-38.831	80.451	17.779	16.169	3.180	143.	-2.409	1.884
12.83000	-38.495	80.214	17.268	15.751	3.259	141.	-2.998	2.224
13.08000	-39.043	79.804	16.815	15.310	3.050	143.	-3.724	2.598
13.33000	-39.748	79.239	16.338	14.918	3.128	141.	-3.224	2.346
13.58000	-40.542	78.320	15.896	14.521	3.067	141.	-3.495	2.485
13.83000	-41.069	77.188	15.470	14.139	3.008	141.	-4.158	2.800
14.08000	-41.098	75.767	15.059	13.768	2.951	141.	-5.795	3.445
14.33000	-40.795	75.132	14.661	13.407	2.897	141.	-7.466	3.955
14.58000	-40.412	74.910	14.273	13.055	2.845	141.	-7.749	4.029
14.83000	-40.116	74.726	13.897	12.713	2.794	141.	-8.649	4.247
15.08000	-39.707	74.845	13.533	12.382	2.746	141.	-6.990	3.822
15.33000	-40.173	73.732	13.180	12.060	2.699	141.	-5.966	3.504
15.58000	-40.720	72.751	12.838	11.747	2.654	141.	-4.882	3.106
15.83000	-41.081	72.029	12.503	11.440	2.610	141.	-3.464	2.470
16.08000	-41.635	70.851	12.178	11.141	2.568	141.	-2.966	2.207

BSS, RL vs. time

ORIGINAL PROCESSING | 1-s CW

Fig. 9 (cont.) – For the original processing of CST-5 Run 1B data, printout of various direct-path processing input parameters and output values as a function of time for the 1-s CWs. Selected times have been chosen from the original file.

CST-5 Run 1B *SA_56.INP* File

Bottom Area

	Generic File	Bottom Bounces	Surface Bounces	Beamformer File	Tilt Angle
VLA	EIGRAS	0	0	SRCBP	4.00
HLA	EIGRAR	0	0	RCVBP	0.00

Start Time	Stop Time	Pulse Width	Pulse Width Increments
0.580	20.580	1.000	4

Distance between arrays in km 0.8808000
Horizontal MRA in degrees 138.2500
Vertical MRA in degrees 25.00000

Time	Effective Area(dB)	HLA Grazing	VLA Grazing	HLA Bearing	Bistatic Angle
7.330	-118.999	36.627	31.488	163.000	2.896
7.580	-118.816	35.011	30.290	159.000	3.399
7.830	-117.885	32.590	29.919	120.999	8.044
8.080	-115.994	32.239	28.061	158.999	3.129
8.330	-114.670	30.911	27.125	152.999	3.827
8.580	-111.479	29.723	26.201	150.999	3.944
8.830	-109.179	28.609	25.332	148.999	4.051
9.080	-107.394	27.595	24.485	148.999	3.917
9.330	-106.283	26.615	23.714	146.999	4.016
9.580	-104.965	25.721	22.960	146.999	3.893
9.830	-103.715	24.874	22.241	146.999	3.779
10.080	-102.638	24.071	21.558	146.999	3.671
10.330	-101.913	23.280	20.929	144.999	3.764
10.580	-101.507	22.555	20.304	144.999	3.664
10.830	-101.289	21.861	19.705	144.999	3.569
11.080	-101.156	21.177	19.157	143.000	3.654
11.330	-101.011	20.552	18.611	143.000	3.565
11.580	-101.139	19.952	18.085	143.000	3.480
11.830	-101.498	19.375	17.578	143.000	3.400
12.080	-102.208	18.822	17.090	142.999	3.323
12.330	-103.237	18.289	16.621	142.999	3.250
12.580	-104.218	17.779	16.169	143.000	3.180
12.830	-104.791	17.268	15.751	141.000	3.259
13.080	-104.653	16.815	15.310	143.000	3.050
13.330	-104.513	16.338	14.918	141.000	3.128
13.580	-104.638	15.896	14.521	141.000	3.067
13.830	-105.243	15.470	14.139	141.000	3.008
14.080	-106.635	15.059	13.768	141.000	2.951
14.330	-107.573	14.661	13.407	141.000	2.897
14.580	-108.178	14.273	13.055	141.000	2.845
14.830	-108.658	13.897	12.713	141.000	2.794
15.080	-108.948	13.533	12.382	141.000	2.746
15.330	-109.595	13.180	12.060	141.000	2.699
15.580	-110.029	12.838	11.747	141.000	2.654
15.830	-110.390	12.503	11.440	141.000	2.610
16.080	-111.014	12.178	11.141	141.000	2.568

WA vs. time

ORIGINAL PROCESSING | 1-s CW

Fig. 9 (cont.) – For the original processing of CST-5 Run 1B data, printout of various direct-path processing input parameters and output values as a function of time for the 1-s CWs. Selected times have been chosen from the original file.

CST-5 Run 1B *DP_56.DAT* File

CST RUN # 1I
DATA FILE: DP_56.DAT
NUMBER OF BEAMS = 64, NUMBER OF PINGS ENSEMBLE AVERAGED = 19
SOURCE LEVEL = 226.0 DB, START TIME = 161:02:17:06.09 ← **NOTE: SL value**
WEIGHTED AREA FILE: SA_56.OUT
VLA STEERING = -25.00, HLA STEERING = 138.25
NUMBER OF POINTS = 320 CENTER FREQUENCY = 935.

TIME	BACKSCAT	REVERB	S. GRAZE	I. GRAZE	BIANGLE	HLA BEAR	RVB-STD	RVB+STD
12.45500	-47.773	69.095	17.945	16.301	3.236	143.	-5.499	3.341
12.51750	-47.119	69.719	17.815	16.186	3.220	143.	-6.512	3.680
12.58000	-47.027	69.976	17.668	16.094	3.351	141.	-6.428	3.654
12.64250	-47.132	69.721	17.565	15.963	3.184	143.	-5.579	3.370
12.70500	-47.556	69.291	17.443	15.855	3.167	143.	-4.946	3.132
12.76750	-47.899	68.910	17.319	15.746	3.151	143.	-4.247	2.840
12.83000	-47.832	68.580	17.196	15.637	3.134	143.	-3.945	2.703
12.89250	-47.587	68.347	17.075	15.528	3.119	143.	-3.524	2.500
12.95500	-47.904	67.661	16.938	15.442	3.246	141.	-3.030	2.242
13.01750	-48.809	66.850	16.819	15.337	3.229	141.	-2.796	2.112
13.08000	-49.496	66.493	16.702	15.233	3.213	141.	-2.949	2.197
13.14250	-50.150	66.004	16.584	15.128	3.196	141.	-3.322	2.397
13.20500	-49.740	66.317	16.471	15.025	3.180	141.	-3.329	2.401
13.26750	-48.817	66.743	16.358	14.923	3.163	141.	-3.203	2.335
13.33000	-48.317	66.772	16.266	14.807	3.008	143.	-3.723	2.598
13.39250	-48.359	66.936	16.152	14.705	2.994	143.	-3.771	2.621
13.45500	-47.947	67.053	16.022	14.624	3.117	141.	-3.439	2.457
13.51750	-48.016	66.852	15.912	14.523	3.100	141.	-3.409	2.442
13.58000	-48.306	66.419	15.823	14.410	2.948	143.	-3.532	2.504
13.64250	-48.141	66.016	15.696	14.329	3.071	141.	-3.938	2.700
13.70500	-48.446	65.874	15.588	14.234	3.056	141.	-4.525	2.960
13.76750	-48.756	65.710	15.480	14.136	3.041	141.	-4.561	2.975
13.83000	-48.669	65.487	15.377	14.042	3.026	141.	-4.860	3.098
13.89250	-48.471	65.252	15.272	13.948	3.012	141.	-5.790	3.443
13.95500	-48.735	64.493	15.170	13.856	2.998	141.	-6.096	3.547
14.01750	-48.612	64.238	15.066	13.763	2.983	141.	-5.521	3.349
14.08000	-48.104	64.541	14.964	13.671	2.969	141.	-4.364	2.891
14.14250	-48.186	64.319	14.863	13.578	2.955	141.	-4.314	2.869
14.20500	-48.184	64.223	14.764	13.489	2.942	141.	-4.616	2.998
14.26750	-48.181	64.210	14.663	13.398	2.928	141.	-4.991	3.150
14.33000	-48.867	63.873	14.565	13.310	2.914	141.	-5.294	3.265
14.39250	-49.405	63.637	14.465	13.220	2.901	141.	-5.423	3.313
14.45500	-49.721	63.372	14.370	13.132	2.888	141.	-6.441	3.658
14.51750	-49.656	63.248	14.274	13.045	2.874	141.	-6.626	3.715
14.58000	-49.740	62.981	14.179	12.959	2.861	141.	-6.626	3.714
14.64250	-49.810	62.725	14.082	12.872	2.848	141.	-6.085	3.543
14.70500	-49.969	62.347	13.988	12.787	2.836	141.	-4.806	3.076
14.76750	-50.191	61.935	13.895	12.701	2.823	141.	-3.824	2.646
14.83000	-49.974	61.833	13.804	12.618	2.811	141.	-4.386	2.901
14.89250	-49.354	62.121	13.710	12.533	2.798	141.	-4.962	3.138
14.95500	-48.672	62.580	13.619	12.451	2.786	141.	-6.106	3.550
15.01750	-48.509	62.712	13.527	12.367	2.774	141.	-6.814	3.771
15.08000	-48.294	62.650	13.439	12.286	2.761	141.	-7.900	4.068

BSS, RL vs. time

ORIGINAL PROCESSING | 0.25-s CW

Fig. 9 (cont.) – For the original processing of CST-5 Run 1B data, printout of various direct-path processing input parameters and output values as a function of time for the 0.25-s CWs. Selected times have been chosen from the original file.

CST-5 Run 1B *SA_56.OUT* File

Bottom Area

	Generic File	Bottom Bounces	Surface Bounces	Beamformer File	Tilt Angle
VLA	EIGRAS	0	0	SRCBP	4.00
HLA	EIGRAR	0	0	RCVBP	0.00

Start Time	Stop Time	Pulse Width	Pulse Width Increments
0.580	20.580	0.250	4

Distance between arrays in km 0.8808000
Horizontal MRA in degrees 138.2500
Vertical MRA in degrees 25.00000

Time	Effective Area(dB)	HLA Grazing	VLA Grazing	HLA Bearing	Bistatic Angle
12.455	-109.132	17.945	16.301	143.000	3.236
12.517	-109.163	17.816	16.187	142.999	3.219
12.580	-108.997	17.668	16.094	141.000	3.351
12.642	-109.147	17.566	15.964	143.000	3.184
12.705	-109.153	17.443	15.855	143.000	3.167
12.767	-109.188	17.320	15.747	143.000	3.151
12.830	-109.588	17.196	15.637	143.000	3.134
12.892	-110.063	17.076	15.529	142.999	3.118
12.955	-110.435	16.938	15.442	141.000	3.246
13.017	-110.344	16.820	15.338	141.000	3.229
13.080	-110.011	16.702	15.233	141.000	3.213
13.142	-109.845	16.585	15.129	141.000	3.196
13.205	-109.943	16.471	15.025	141.000	3.180
13.267	-110.436	16.359	14.924	141.000	3.164
13.330	-110.911	16.266	14.807	143.000	3.008
13.392	-110.703	16.153	14.706	143.000	2.993
13.455	-111.000	16.022	14.624	141.000	3.117
13.517	-111.131	15.913	14.524	141.000	3.101
13.580	-111.275	15.823	14.410	143.000	2.948
13.642	-111.844	15.697	14.330	141.000	3.071
13.705	-111.680	15.588	14.234	141.000	3.056
13.767	-111.532	15.481	14.137	141.000	3.041
13.830	-111.844	15.377	14.042	141.000	3.026
13.892	-112.273	15.273	13.949	141.000	3.012
13.955	-112.772	15.170	13.856	141.000	2.998
14.017	-113.149	15.067	13.764	141.000	2.983
14.080	-113.355	14.964	13.671	141.000	2.969
14.142	-113.494	14.864	13.579	141.000	2.955
14.205	-113.593	14.764	13.489	141.000	2.942
14.267	-113.611	14.664	13.399	141.000	2.928
14.330	-113.260	14.565	13.310	141.000	2.914
14.392	-112.959	14.466	13.221	141.000	2.901
14.455	-112.907	14.370	13.132	141.000	2.888
14.517	-113.095	14.275	13.046	141.000	2.874
14.580	-113.279	14.179	12.959	141.000	2.861
14.642	-113.463	14.083	12.873	141.000	2.848
14.705	-113.684	13.988	12.787	141.000	2.836
14.767	-113.871	13.896	12.702	141.000	2.823
14.830	-114.193	13.804	12.618	141.000	2.811
14.892	-114.523	13.711	12.534	141.000	2.798
14.955	-114.748	13.619	12.451	141.000	2.786
15.017	-114.777	13.528	12.368	141.000	2.774
15.080	-115.056	13.439	12.286	141.000	2.761

WA vs. time

ORIGINAL PROCESSING | 0.25-s CW

Fig. 9 (cont.) – For the original processing of CST-5 Run 1B data, printout of various direct-path processing input parameters and output values as a function of time for the 0.25-s CWs. Selected times have been chosen from the original file.

TIME INTERPOLATION PRINT FILE FOR PROGRAM DP_MATCH_RAYS_BEAM

EXPERIMENT: CST5 PING SET RUN HF EPOCH 1

SOURCE DEPTH = 130.00 m
RECEIVER DEPTH = 138.00 m
BOTTOM DEPTH = 3440.00 m

SOURCE-RECEIVER SEPARATION OF -880.0 m = -0.5 n mi
(negative if geometry is ship:source:receiver)

TILT = 4.00 deg
KITE = 0.00 deg
STEERANGLE = -25.00 deg

TIME RESOLUTION = 0.10 sec
ANALYSIS TIME = 1.00 sec
PING DURATION = 1.00 sec

BEAM NO. 8 BEAM ANGLE = 138.6 deg.
(0 deg is toward ship, 90 deg is broadside.)

TIME (S)	RANGE SRC (M)	RCV (M)	ALPHA (DEG)	TL (dB)	GRAZ-ANG SRC (deg)	RCV (deg)	MEAN ANG (deg)	BIST ANG (deg)	AREA (dB)	DB DN
7.35	5007.0	4146.5	166.7	-150.0	31.9	37.3	34.6	6.7	62.3	-20.0
7.55	5192.8	4345.0	163.0	-150.5	30.9	35.9	33.4	6.4	61.3	-20.0
7.86	5468.1	4636.7	159.2	-151.1	29.5	34.0	31.8	6.1	60.6	-20.0
8.06	5649.5	4827.6	157.3	-151.6	28.6	32.9	30.8	5.9	60.4	-20.0
8.36	5919.1	5109.7	155.0	-152.2	27.4	31.3	29.4	5.6	60.2	-20.0
8.57	6097.1	5295.2	153.8	-152.6	26.6	30.3	28.5	5.5	60.1	-20.0
8.87	6362.1	5570.1	152.3	-153.2	25.5	29.0	27.2	5.2	60.0	-20.0
9.07	6537.5	5751.2	151.4	-153.6	24.8	28.1	26.5	5.1	60.0	-19.3
9.38	6798.9	6020.6	150.3	-154.2	23.9	26.9	25.4	4.9	60.0	-16.3
9.58	6972.0	6198.6	149.6	-154.6	23.3	26.1	24.7	4.8	60.0	-14.5
9.79	7144.4	6375.4	149.0	-154.9	22.7	25.4	24.0	4.7	60.1	-13.0
10.09	7401.6	6638.7	148.3	-155.5	21.8	24.4	23.1	4.5	60.1	-11.1
10.29	7572.3	6813.1	147.8	-155.8	21.3	23.8	22.5	4.4	60.1	-10.1
10.60	7827.2	7073.1	147.2	-156.3	20.5	22.9	21.7	4.3	60.2	-8.9
10.80	7996.5	7245.4	146.8	-156.6	20.0	22.3	21.2	4.2	60.3	-8.2
11.11	8249.4	7502.7	146.3	-157.1	19.3	21.4	20.4	4.0	60.3	-7.4
11.31	8417.4	7673.3	146.0	-157.4	18.9	20.9	19.9	4.0	60.4	-7.0
11.61	8668.7	7928.4	145.6	-157.9	18.2	20.2	19.2	3.9	60.5	-6.5
11.82	8835.7	8097.6	145.4	-158.2	17.8	19.7	18.8	3.8	60.5	-6.3
12.12	9085.5	8350.6	145.0	-158.6	17.2	19.0	18.1	3.7	60.6	-6.1
12.32	9251.6	8518.7	144.8	-158.9	16.8	18.6	17.7	3.6	60.6	-6.0
12.53	9417.4	8686.4	144.6	-159.2	16.5	18.1	17.3	3.5	60.7	-5.9
12.83	9665.5	8937.1	144.3	-159.6	15.9	17.5	16.7	3.5	60.8	-5.9
13.04	9830.5	9103.8	144.1	-159.8	15.6	17.1	16.4	3.4	60.8	-6.0
13.34	10077.6	9353.2	143.9	-160.2	15.1	16.6	15.8	3.3	60.9	-6.1
13.54	10242.1	9519.1	143.8	-160.5	14.8	16.2	15.5	3.3	61.0	-6.2
13.85	10488.2	9767.2	143.6	-160.9	14.3	15.7	15.0	3.2	61.0	-6.4
14.05	10652.0	9932.4	143.4	-161.1	14.0	15.3	14.7	3.1	61.1	-6.6
14.36	10897.3	10179.4	143.2	-161.5	13.5	14.8	14.2	3.1	61.2	-6.9
14.56	11060.5	10343.9	143.1	-161.7	13.3	14.5	13.9	3.0	61.2	-7.1
14.86	11305.2	10590.2	143.0	-162.1	12.8	14.1	13.4	3.0	61.3	-7.4
15.07	11468.0	10754.0	142.9	-162.3	12.6	13.8	13.2	2.9	61.4	-7.7
15.37	11712.0	10999.5	142.7	-162.6	12.2	13.3	12.7	2.8	61.4	-8.1
15.57	11874.4	11162.8	142.7	-162.9	11.9	13.0	12.5	2.8	61.5	-8.3
15.78	12036.7	11326.0	142.6	-163.1	11.7	12.8	12.2	2.8	61.5	-8.6
16.08	12279.9	11570.5	142.5	-163.4	11.3	12.4	11.8	2.7	61.6	-9.0

REPROCESSING 1-s CW

Fig. 10 – For the reprocessing of CST-5 Run 1B data, printout of various direct-path processing input parameters and output values as a function of time for the 1-s CWs. Selected times have been chosen from the original files.

TIME INTERPOLATION PRINT FILE FOR PROGRAM DP_MATCH_RAYS_BEAM

EXPERIMENT: CST5 PING SET RUN HF EPOCH 1

SOURCE DEPTH = 130.00 m
RECEIVER DEPTH = 138.00 m
BOTTOM DEPTH = 3440.00 m

SOURCE-RECEIVER SEPARATION OF -880.0 m = -0.5 n mi
(negative if geometry is ship:source:receiver)

TILT = 4.00 deg
KITE = 0.00 deg
STEERANGLE = -25.00 deg

TIME RESOLUTION = 0.10 sec
ANALYSIS TIME = 0.25 sec
PING DURATION = 0.25 sec

BEAM NO. 8 BEAM ANGLE = 138.6 deg.
(0 deg is toward ship, 90 deg is broadside.)

TIME (S)	RANGE SRC (M)	RANGE RCV (M)	ALPHA (DEG)	TL (dB)	GRAZ-ANG SRC (deg)	GRAZ-ANG RCV (deg)	MEAN ANG (deg)	BIST ANG (deg)	AREA (dB)	DB DN
12.43	9333.6	8601.6	144.7	-159.0	16.7	18.4	17.5	3.6	54.4	-6.0
12.52	9413.3	8682.2	144.6	-159.1	16.5	18.2	17.3	3.5	54.4	-5.9
12.62	9492.8	8762.6	144.5	-159.3	16.3	18.0	17.1	3.5	54.4	-5.9
12.72	9572.3	8843.0	144.4	-159.4	16.1	17.8	16.9	3.5	54.5	-5.9
12.82	9651.8	8923.3	144.3	-159.5	16.0	17.6	16.8	3.5	54.5	-5.9
12.91	9731.3	9003.5	144.2	-159.7	15.8	17.4	16.6	3.4	54.5	-6.0
13.01	9810.5	9083.6	144.2	-159.8	15.6	17.2	16.4	3.4	54.5	-6.0
13.11	9889.8	9163.6	144.1	-159.9	15.5	17.0	16.2	3.4	54.6	-6.0
13.21	9969.1	9243.7	144.0	-160.1	15.3	16.8	16.1	3.3	54.6	-6.1
13.3010048.2		9323.5	143.9	-160.2	15.1	16.6	15.9	3.3	54.6	-6.1
13.4010127.3		9403.3	143.9	-160.3	15.0	16.5	15.7	3.3	54.6	-6.2
13.5010206.4		9483.1	143.8	-160.4	14.8	16.3	15.6	3.3	54.7	-6.2
13.6010285.4		9562.8	143.7	-160.5	14.7	16.1	15.4	3.2	54.7	-6.3
13.6910364.3		9642.3	143.7	-160.7	14.5	15.9	15.2	3.2	54.7	-6.4
13.7910443.1		9721.8	143.6	-160.8	14.4	15.8	15.1	3.2	54.7	-6.5
13.8910522.0		9801.3	143.5	-160.9	14.2	15.6	14.9	3.2	54.8	-6.5
13.9910600.8		9880.8	143.5	-161.0	14.1	15.4	14.8	3.1	54.8	-6.7
14.0910679.4		9960.0	143.4	-161.2	13.9	15.3	14.6	3.1	54.8	-6.8
14.1810758.010039.2			143.3	-161.3	13.8	15.1	14.5	3.1	54.8	-6.9
14.2810836.710118.4			143.3	-161.4	13.7	15.0	14.3	3.1	54.9	-7.0
14.3810915.310197.6			143.2	-161.5	13.5	14.8	14.2	3.1	54.9	-7.1
14.4810993.810276.7			143.2	-161.6	13.4	14.6	14.0	3.0	54.9	-7.2
14.5711072.210355.6			143.1	-161.7	13.2	14.5	13.9	3.0	54.9	-7.3
14.6711150.610434.6			143.1	-161.8	13.1	14.3	13.7	3.0	55.0	-7.4
14.7711229.110513.5			143.0	-162.0	13.0	14.2	13.6	3.0	55.0	-7.6
14.8711307.510592.5			143.0	-162.1	12.8	14.1	13.4	3.0	55.0	-7.7
14.9611385.810671.3			142.9	-162.2	12.7	13.9	13.3	2.9	55.0	-7.8
15.0611464.010750.0			142.9	-162.3	12.6	13.8	13.2	2.9	55.1	-8.0

REPROCESSING | 0.25-s CW

Fig. 10 (cont.) – For the reprocessing of CST-5 Run 1B data, printout of various direct-path processing input parameters and output values as a function of time for the 0.25-s CWs. Selected times have been chosen from the original files.

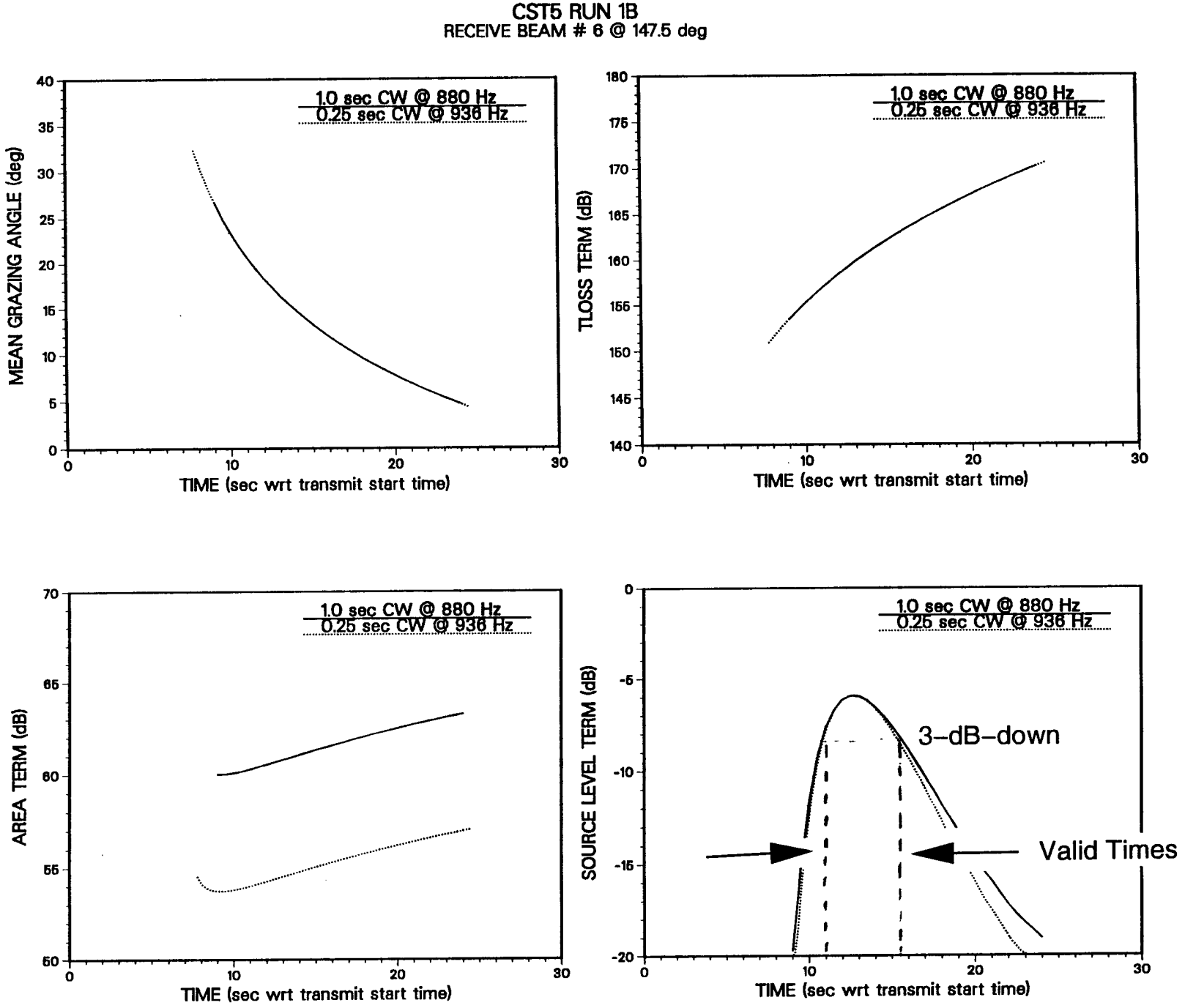

Fig. 11 – For the reprocessed data of CST-5 Run 1B data, various sonar-equation terms as a function of time for the 138° R beam.

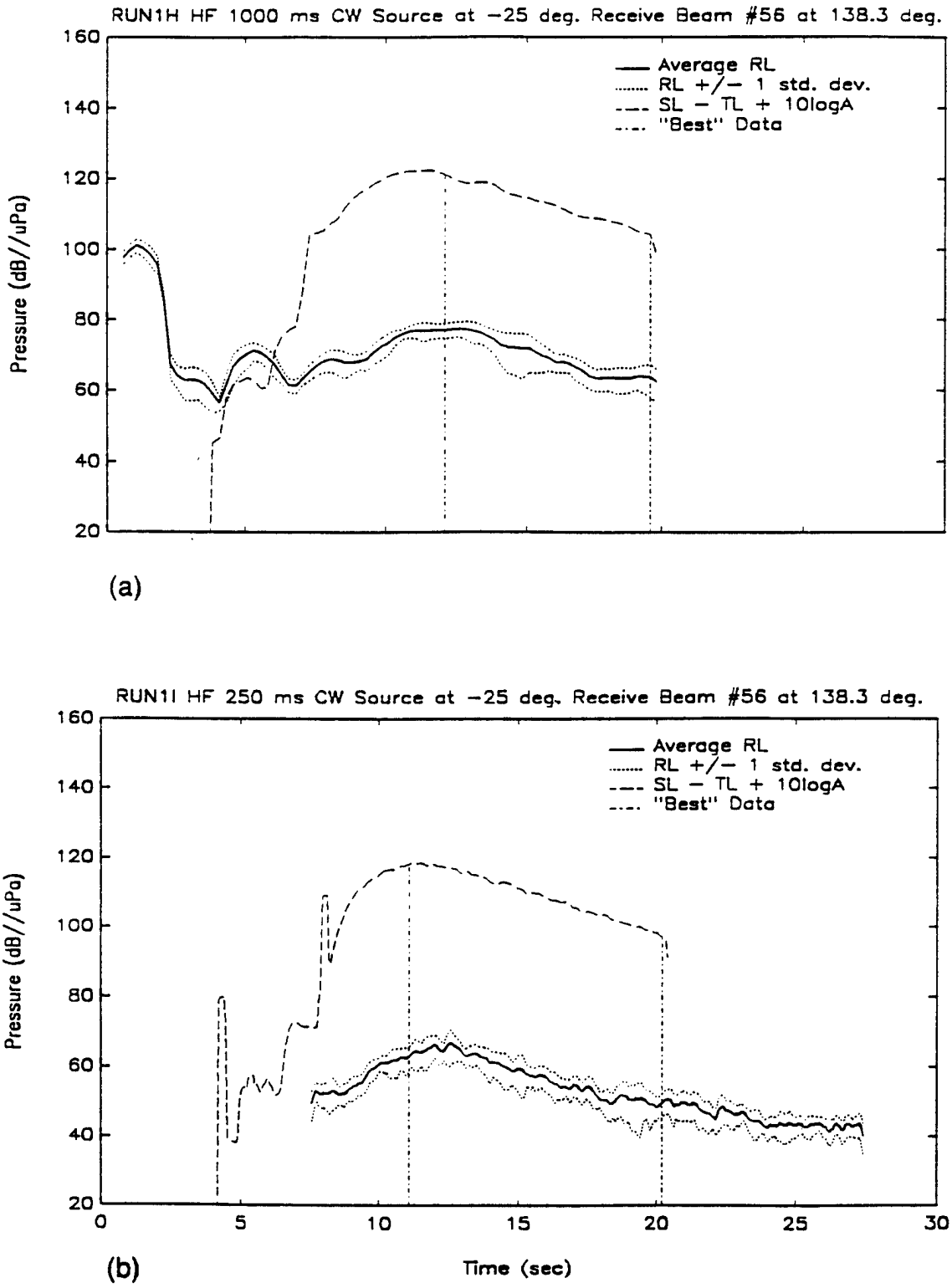

Fig. 12 – RL and SL+WA curves derived in the original processing for the 138°R beam for the (a) 1-s, 880-Hz and (b) 0.25-s, 936-Hz CWs in CST-5 Run 1B. (From Reilly and Sundvik 1992.)

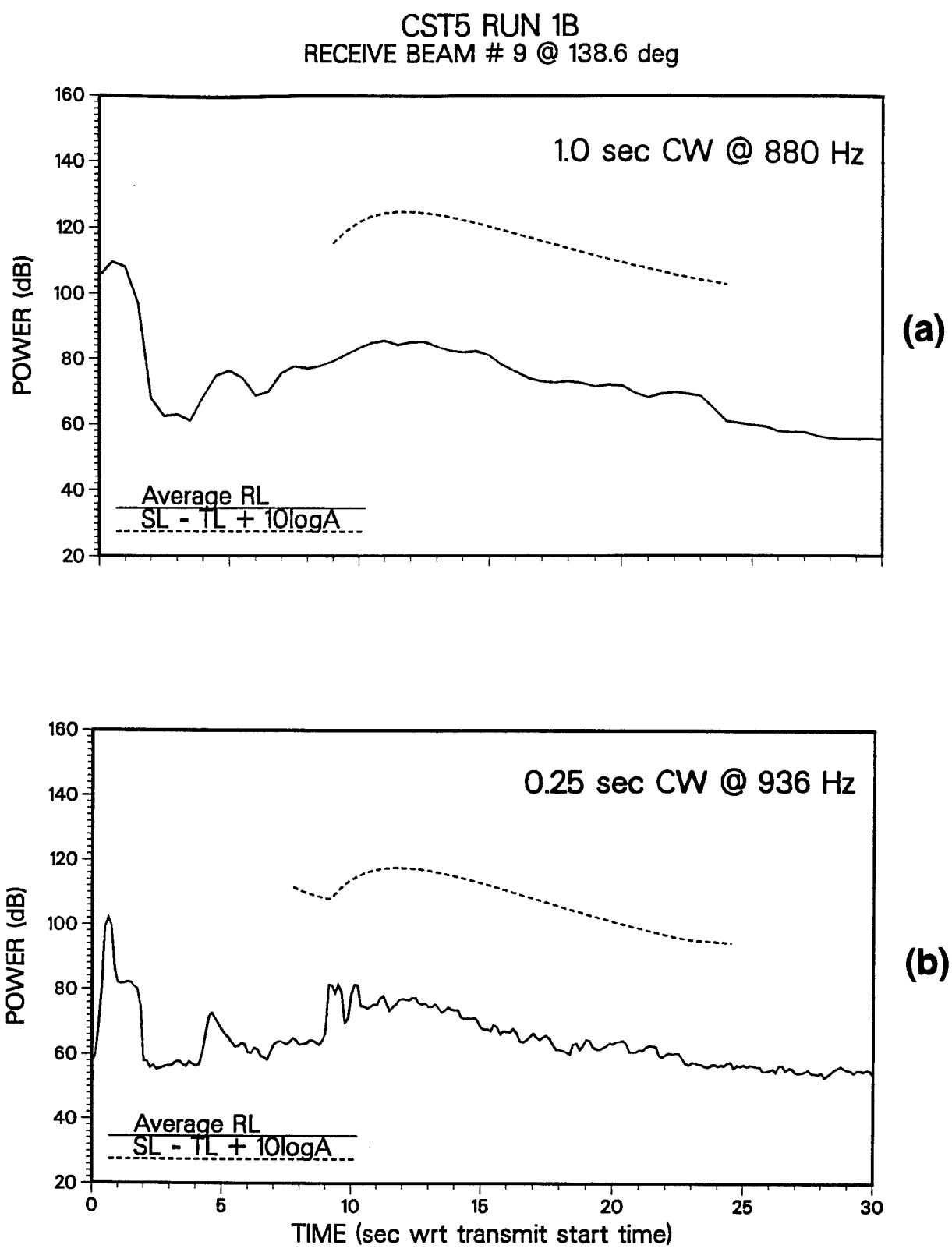

Fig. 13 – RL and SL+WA curves derived in the reprocessing for the 138°R beam for the (a) 1-s, 880-Hz and (b) 0.25-s, 936-Hz CWs in CST-5 Run 1B.

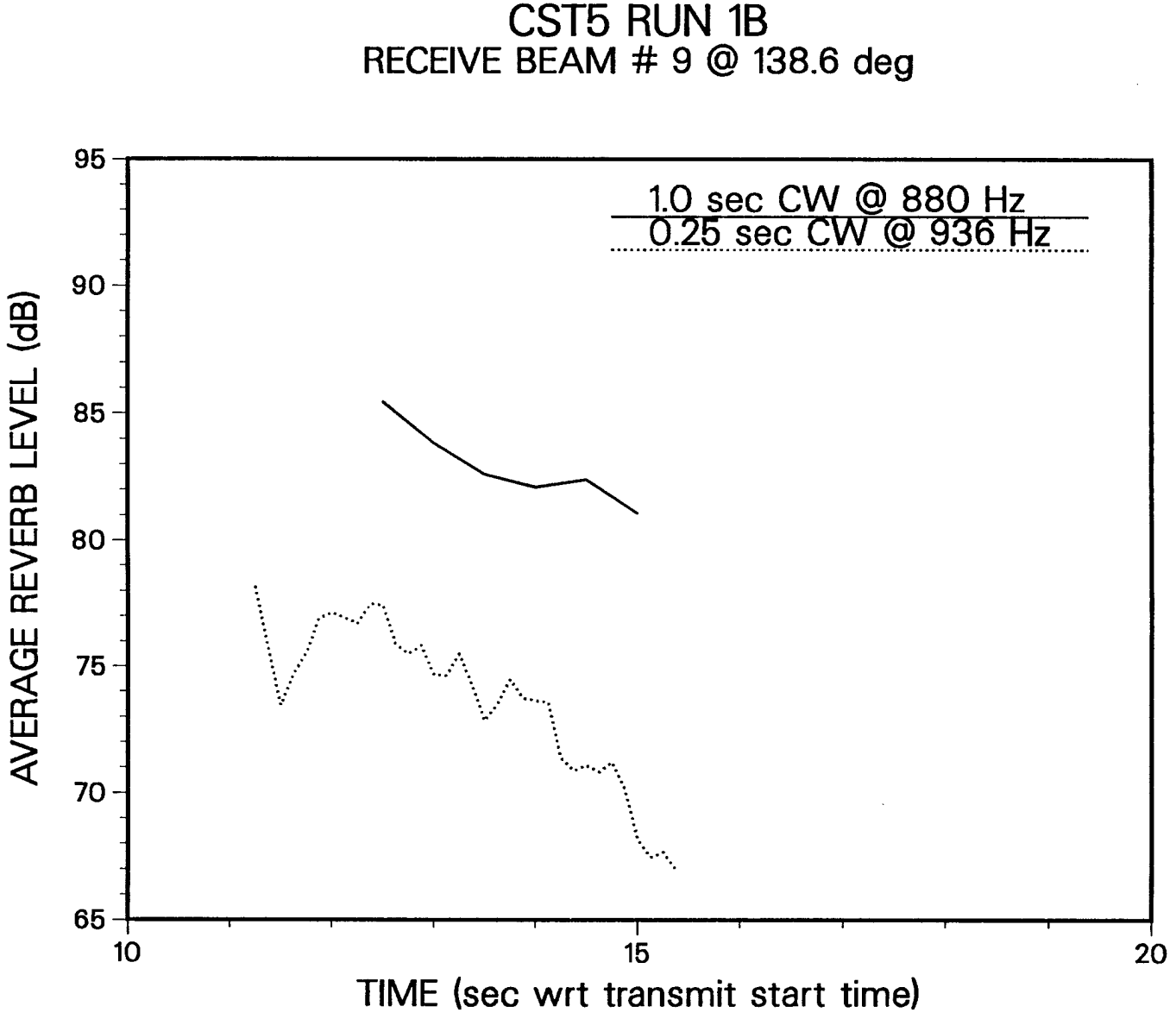

Fig. 14 – RL-NL curves for valid times only derived in the reprocessing. Shown is the 138°R beam for the 1-s, 880-Hz and 0.25-s, 936-Hz CWs.

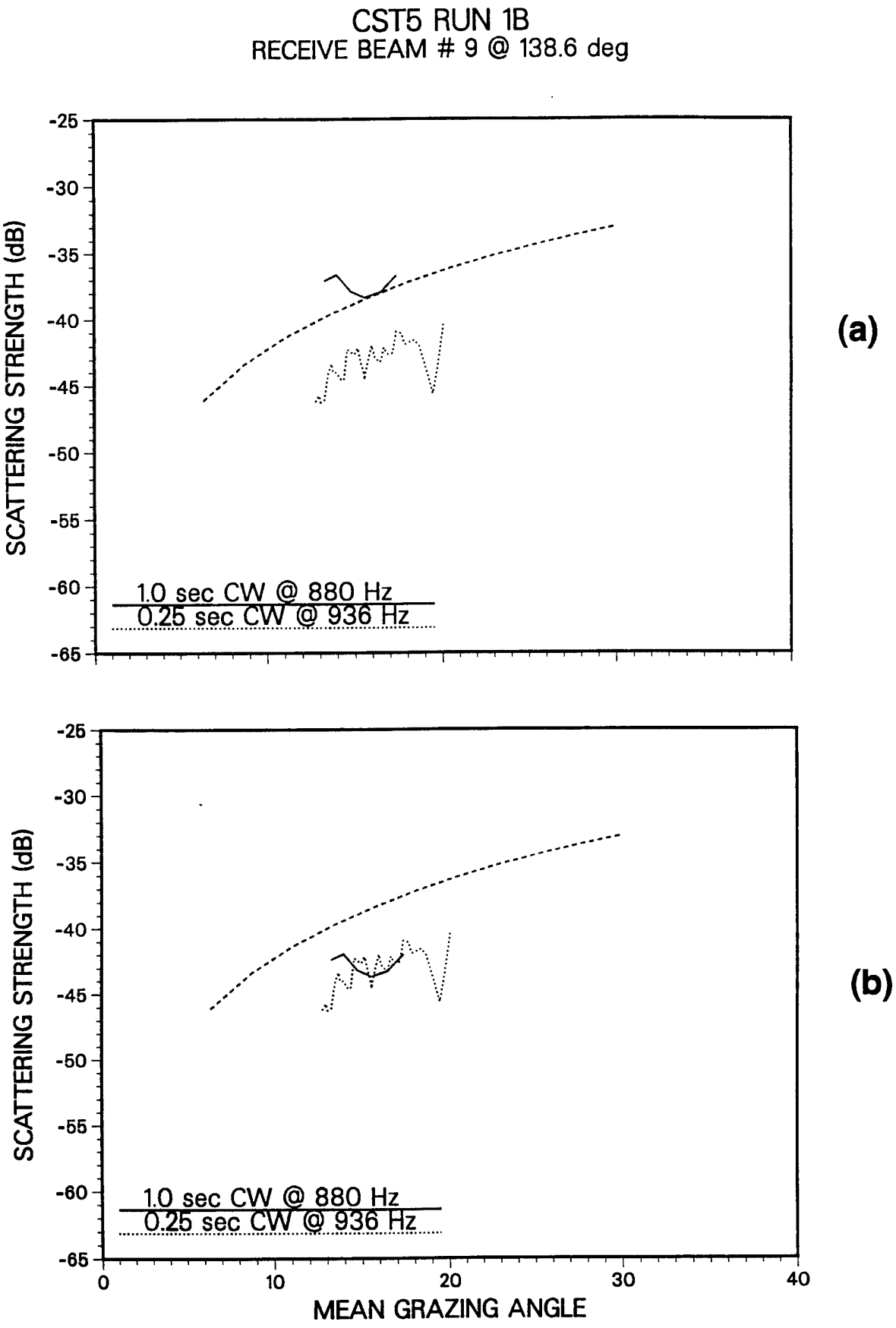

Fig. 15 – Reprocessed CST-5 Run-1B HF BSS's for the 138°R beam using (a) the original SLs and (b) the originally "intended" SLs.

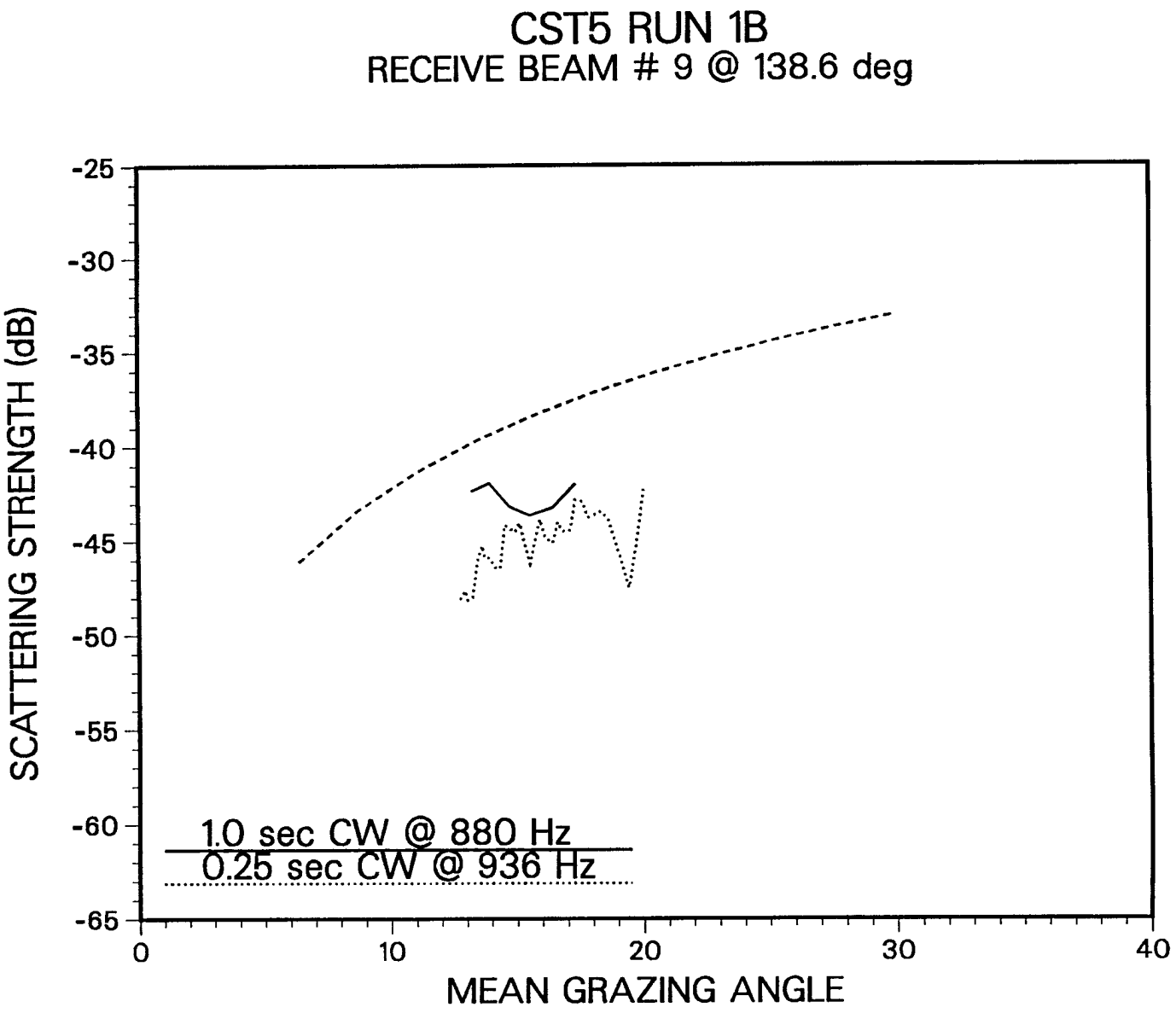

Fig. 16 – Reprocessed CST-5 Run-1B HF BSS's for the 138°R beam using the newly-derived SLs.

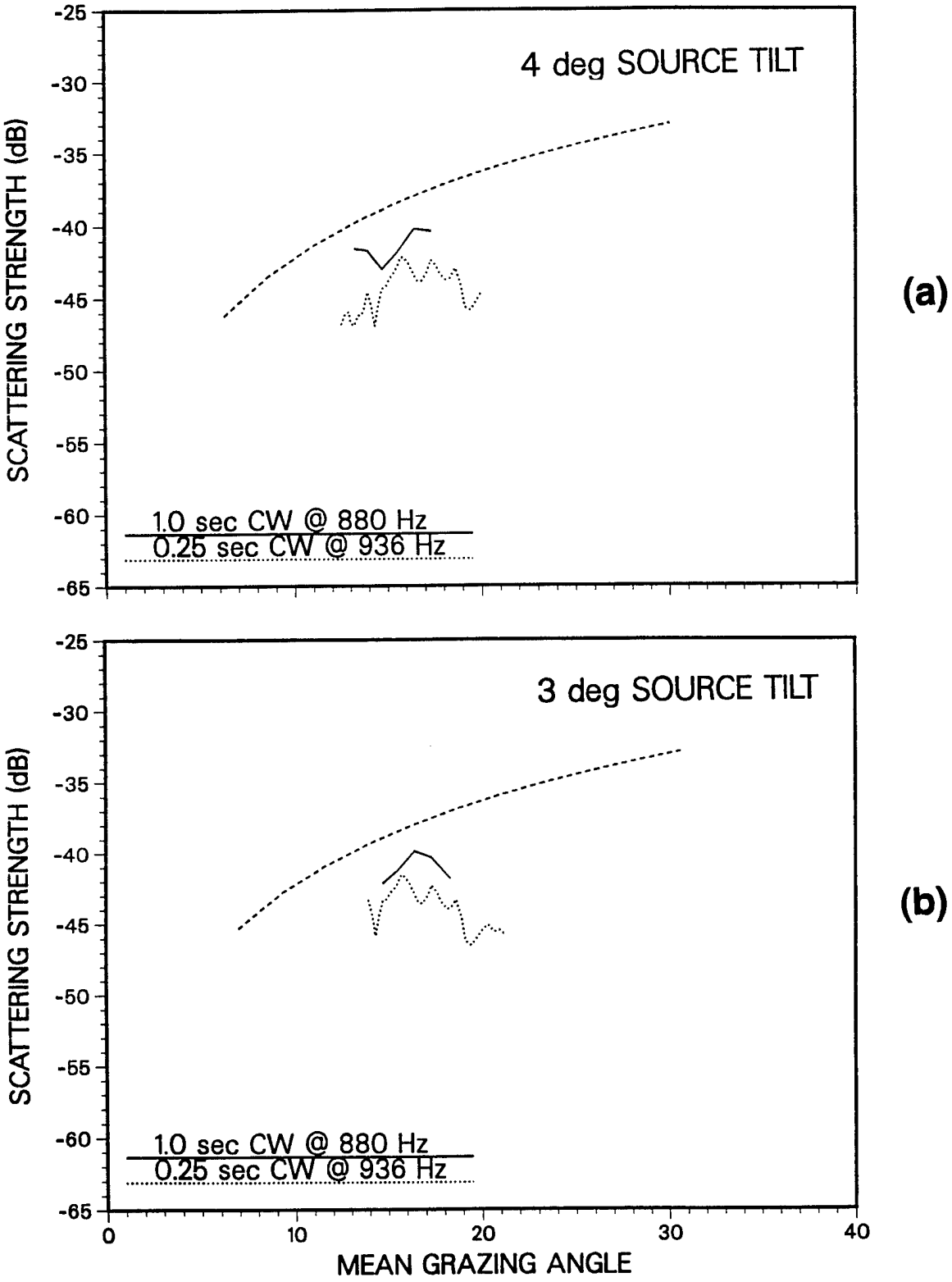

Fig. 17 – Sensitivity to subaperture size and source tilt. Shown are reprocessed CST-5 Run-1B HF BSS's for the 140°R beam using the newly-derived SLs and (a) a 34-phone subaperture and a 4-deg source tilt, and (b) a 34-phone subaperture and a 3-deg source tilt.

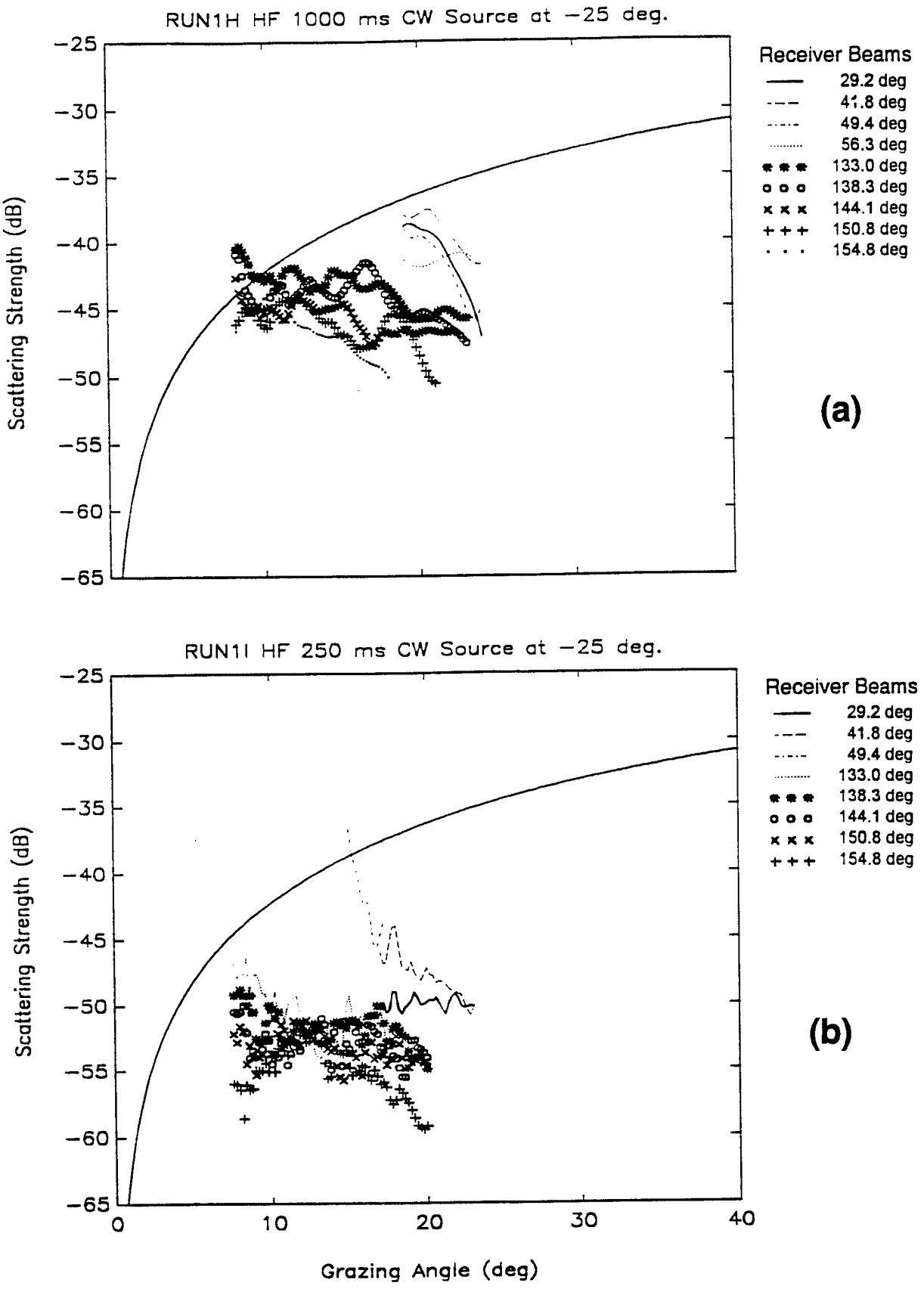

Fig. 18 – Reported CST-5 Run-1B BSS's for various beams for the (a) 1-s, 880-Hz and (b) 0.25-s, 936-Hz CWs. (From Reilly and Sundvik 1992.)

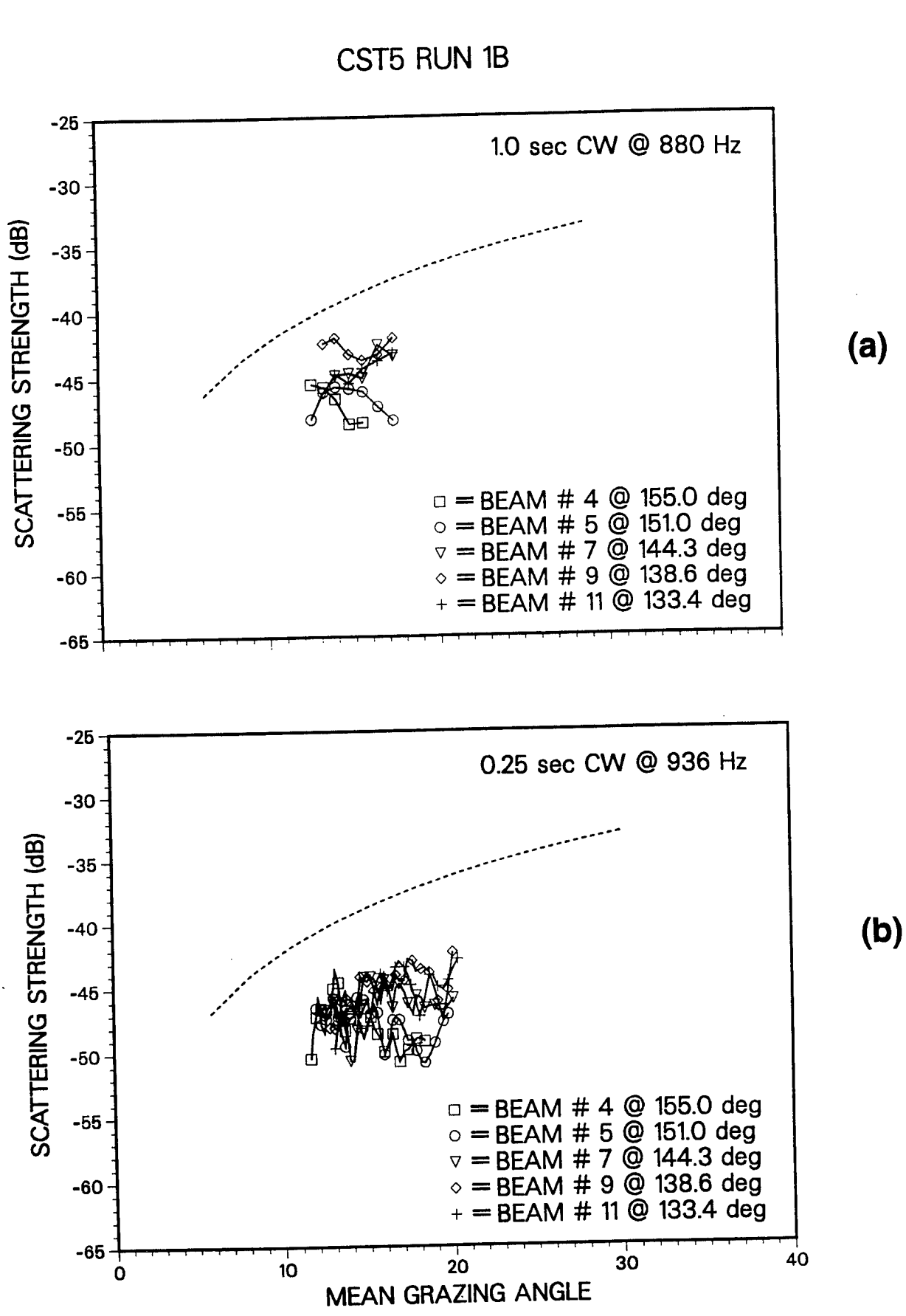

Fig. 19 – Reprocessed CST-5 Run-1B BSS's using the newly-derived SLs for various beams for the (a) 1-s, 880-Hz and (b) 0.25-s, 936-Hz CWs.

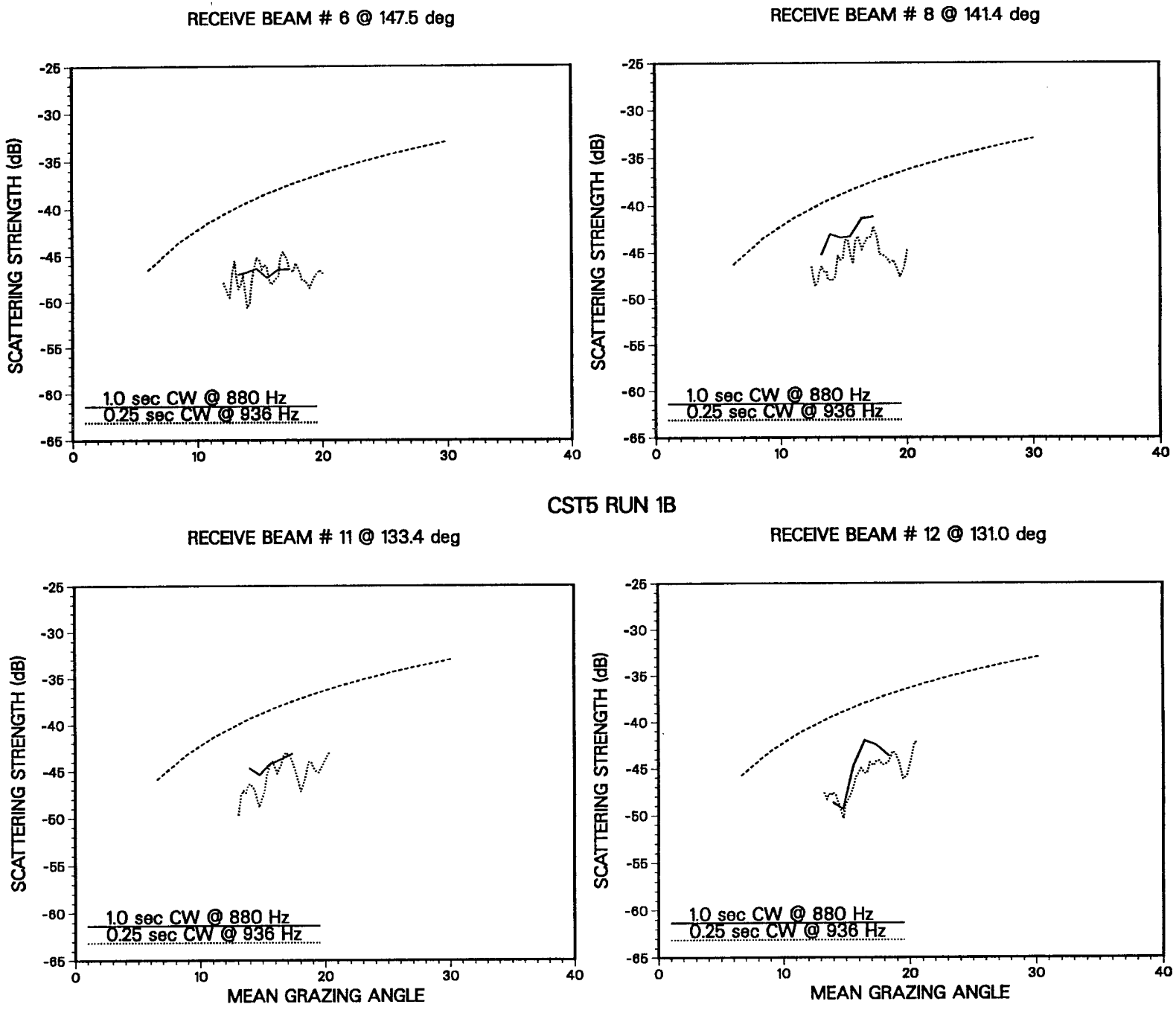

Fig. 20 – Comparison of reprocessed CST-5 Run-1B, HF 0.25- and 1-s–CW BSS's for selected beams (using the newly-derived SLs).

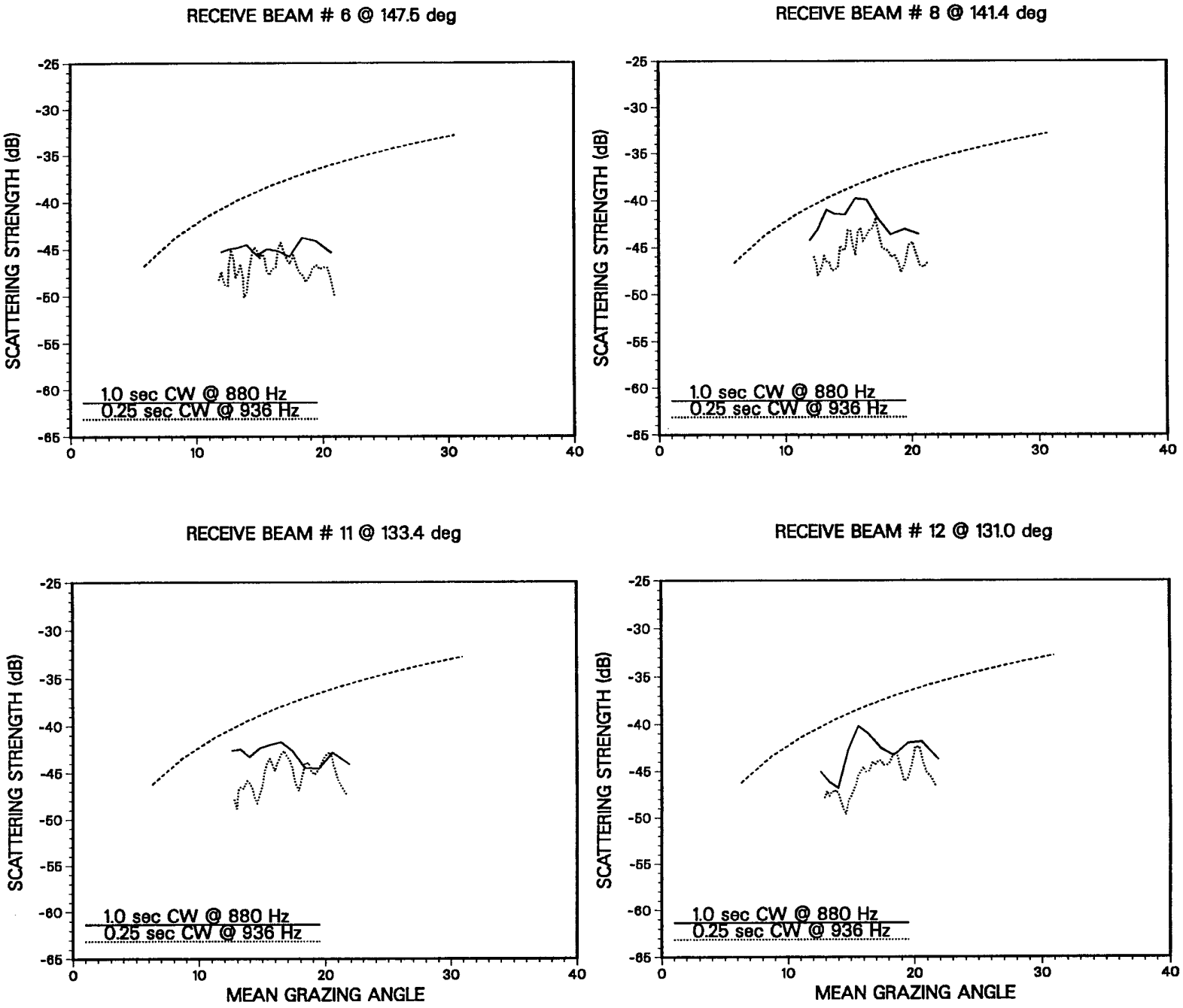

Fig. 21 – Reprocessed CST-5 Run-1B HF BSS's for the 0.25- and 1-s CWs for selected beams for timing differences of -0.25 and -1.0 s, respectively. (These are using the newly-derived SLs.)

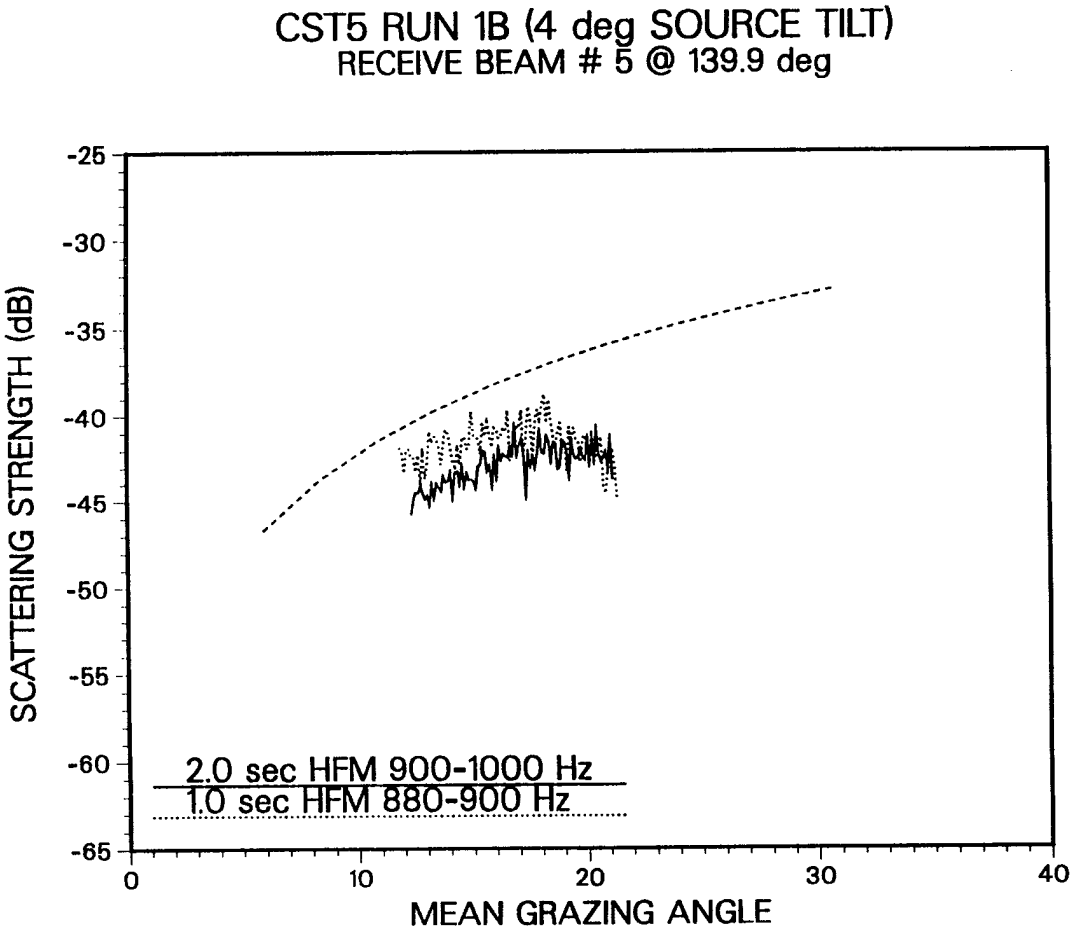

Fig. 22 – Reprocessed CST-5 Run-1B HF BSS's derived from 1-s and 2-s HFM data.

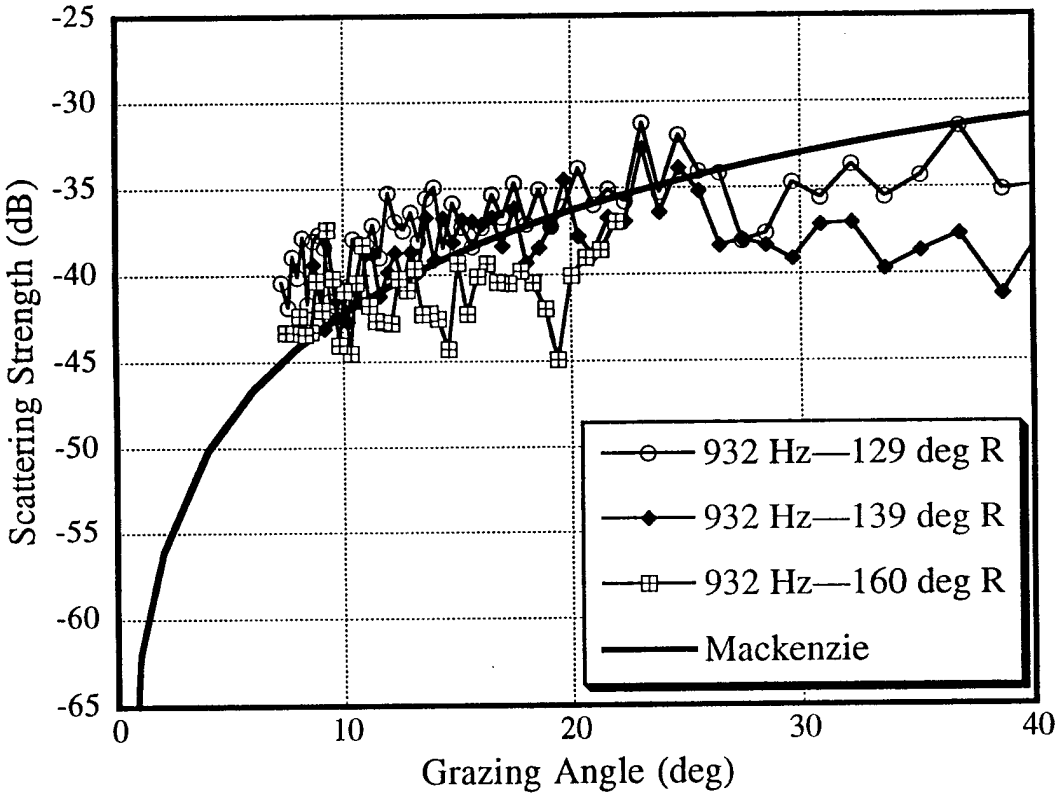

Fig. 23 – CST-5 HF BSS's derived using adaptive beamforming on Run-2 SUS data.

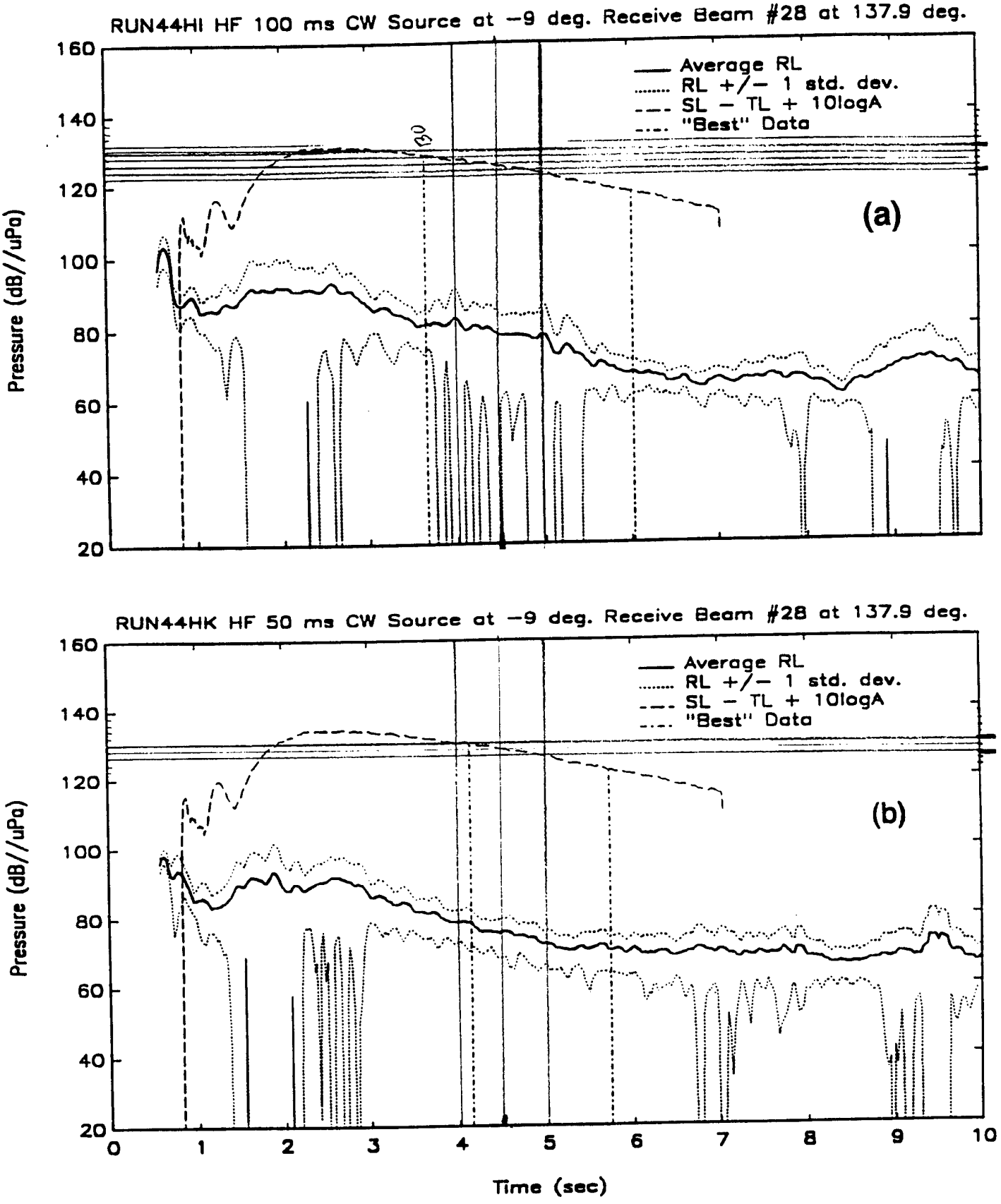

Fig. 24 – CST-5 Run-44 RL and SL+WA curves derived in the original processing for the 138°R beam for the (a) 0.1-s, 1004-Hz and (b) 0.05-s, 935-Hz CWs. (From Reilly and Sundvik 1992.)

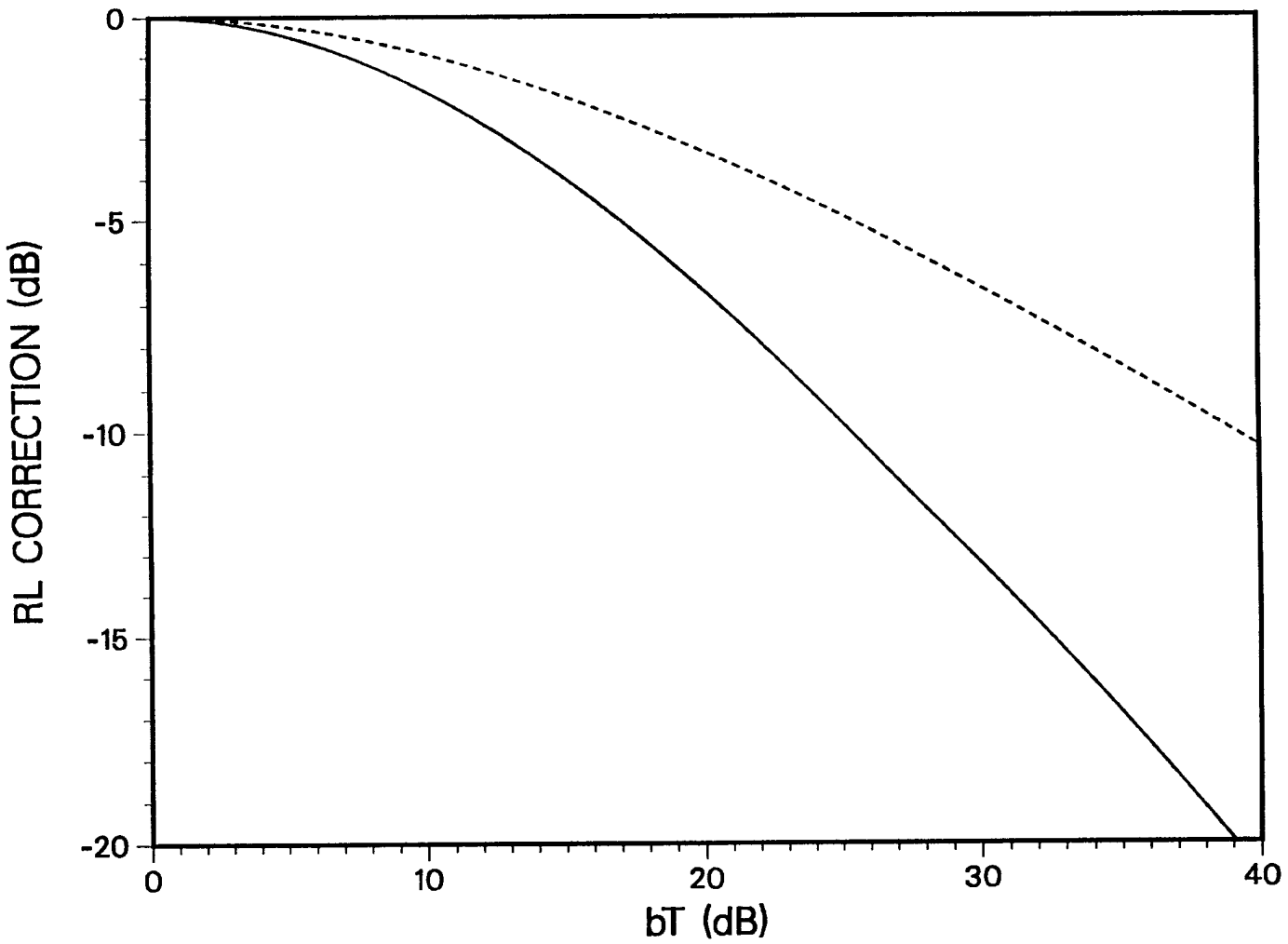

Fig. 25 – The effect of a long pulse if the receive level changes rapidly. Shown is required RL correction versus the receive-level change over a time T. (Here b represents the local slope of the reverberation-decay curve in dB/s.) The solid curve represents the case where the processing resolution is matched to the pulse duration of T s. The dashed curve represents the case where an impulsive signal is processed with a T-s window. (Adapted from Fig. 2 in Henyey *et al.* 1996.)